Ground state and dynamic structure of quantum fluids

M. Saarela
Dept. of Physical Sciences, P.O. Box 3000, FIN-90014 University of Oulu, Finland
E-mail: Mikko.Saarela@oulu.fi

December 11, 2008

Lecture notes at fall 2008, University of Oulu
Material for reading:
A. Fabrocini, S. Fantoni, and E. Krotscheck (Eds.):
Introduction to Modern Methods of
Quantum Many-Body Theories and
Their Applications
Series on Advances in Quantum Many-Body Theory - Vol. 7,
World Scientific, London, 2002

Contents

1 Historical background **1**
1.1 General Properties of liquid helium 3

2 Microscopic description **5**
2.1 General properties of the ground state 11

3 Hypernetted–chain equations **13**

4 Optimized ground state **23**
4.1 Euler equation with the Jastrow wave function 25

5 Dynamic structure of Bose fluids **30**
5.1 Low excited states 31
5.2 Linear response and equation of motion method 36
5.3 Time–dependent correlation functions 40
5.4 Action integral 41
5.5 Least action principle 43
5.6 Many–particle densities and currents 43
5.7 One– and two–particle continuity equations 44

6 Solving the continuity equations **46**
6.1 Feynman approximation 46

7 CBF–approximation **49**
7.1 Convolution approximation 50
7.2 One–particle equation 51
7.3 Two–particle equation 52
7.4 The self–energy and the linear response function 55
7.5 Numerical evaluation of the self–energy 56

8 Summary **58**

List of Figures

1 Schematic phase diagram of liquid ^{4}He in the PT plane. 4
2 Comparison of potentials 7
3 Some cluster diagrams 15
4 Classification of cluster diagrams 16
5 Construction of nodal and composite diagrams 18
6 Chain operations 18
7 Diagrammatic contents of $\exp[N(r)]$. 20
8 Iterative scheme to solve the HNC equations 21
9 Elementary diagrams 22
10 Radial distribution functions 29
11 Static structure functions 30
12 Experimental setup of neutron scattering experiments 33
13 Convolution approximation 51
14 $S(k, w)$ for helium at the saturation density. 58
15 $S(k, w)$ for a hard core potential at $x = 0.1$. 59

1 Historical background

The liquefaction of helium by Kammerlingh Onnes (1908) [1] signaled the birth of *modern low–temperature physics*. Since then, atomic helium fluids became an endless source of physical motivations for both theorists and experimentalists and have played a crucial role in the evolution of low temperature physics during the last century.

Helium is the lightest element of the *noble gases* and has two stable isotopes: ^{4}He and ^{3}He, the former being a 99.99986% of the total population. The atomic structure of the He atom is very simple, having two electrons in the $1s$ orbital in a spin singlet state around a nucleus, composed of two protons and two neutrons in the case of the ^{4}He, and two protons and one neutron for ^{3}He. As the number of fermionic constituents of the ^{4}He atom is even, its total spin is integer and therefore it behaves as a boson. On the other hand, the number of fermionic constituents in ^{3}He is odd, its total spin is 1/2 and it behaves as a fermion.

The different *statistical character* of the two helium isotopes produces dramatic differences in their physical properties. So far, a huge amount of experimental information on helium liquids has already been accumulated, including precise knowledge of the equation of state and most of its thermodynamic properties. [2, 3, 4] In addition, the dynamics and the excitation spectrum have also been systematically investigated by inelastic neutron scattering. [5]

One of the most remarkable facts is the *phase transition* that takes place in liquid ^{4}He at 2.17 K at saturated vapor pressure. When the liquid is cooled below this temperature, its *viscosity drops to almost zero* and it is able to flow freely through very narrow capillary tubes in such a way that the velocity becomes independent of the pressure gradient along the channel, as it was first shown by Kapitza in 1938. [6]

Under these conditions, liquid ^{4}He not only shows this *super flow* property but also becomes a surprisingly good heat conductor. One of the most spectacular effects where both properties are manifested is the so called *fountain effect*, discovered by Allan and Jones in 1938. [7]

Superfluidity in liquid ^{3}He was discovered much later in 1972 [8] by Osheroff, Lee and Richardson. In this case the transition occurs at 2 mK, a temperature three orders of magnitude smaller than the transition temperature of pure ^{4}He.

Nowadays, great activity concerning helium is concentrated on the possibility a *supersolid phase* and to the condensation of bosons to the lowest quantum state. Elementary exitation modes are well studied, but no theory exists for the full dynamic structure. New ideas for the phase transitions have been developed etc. Helium offers excellent material to study the dependence on dimensionality and the effects of confining geometries on the quantum behavior of those liquids.

For theoreticians helium liquids can be considered as excellent laboratories to study the *quantum many–body problem* and to test and develop many–body theories. This is quite relevant because, in some sense, nearly all branches of physics deal with many–body physics at the most microscopic level of understanding.

The energy and length scales relevant to describe helium liquids define the

atoms as the *microscopic constituents* of our system. Besides, the interaction among the atoms is simple, depends only on the distance, and is well known. In addition, the quantum behavior has macroscopic manifestations and the effects of having different statistics can be investigated.

Actually, the fact that helium remains liquid at zero temperature is a consequence of the *large zero point motion* of the atoms in the fluid and can be considered as a macroscopic quantum effect. Moreover the superfluid behavior is a clear macroscopic manifestation of its quantum nature.

Helium liquids can be considered in the bulk limit but also in *surfaces*. Besides and as mentioned above, almost two–dimensional and one–dimensional realizations are also possible. In addition, droplets of ^{4}He or ^{3}He allow to study the dependence of properties on the number of particles. Actually *helium clusters* is another very interesting field which has evolved very quickly, and the present experimental capabilities make possible to investigate problems as the minimum number of atoms in a cluster required to have superfluidity. [11] Also the existence of the *^{3}He-^{4}He mixtures* permits the study of different types of excitations and the interplay of the correlations and statistics on the excitation spectrum.

Quantum mechanics is the natural tool to describe helium liquids. Indeed, helium liquids at low temperature are *quantum fluids*, which differ from classical fluids in the sense that they can not be described in the framework of classical statistical physics. In a quantum fluid, the thermal de Broglie wavelength is of the order of the mean interparticle distance, and therefore there can be large overlaps between the wave functions of different atoms. In this situation quantum statistics has important consequences and one expects to find large differences between liquid ^{4}He and liquid ^{3}He at low temperatures.

In these lectures, an introduction to the *microscopic description of quantum fluids at zero temperature* is presented. I concentrate on the description of the ground state, although the spectrum of elementary excitations and impurities are also analyzed. Methodological aspects are overemphasized, as the techniques explained can be used in general to describe strongly correlated systems, *i.e.,* systems which can not be properly described by mean field theories and that require the full machinery of the Quantum Many Body Methods (QMBM) to understand their behavior.

I will follow closely the book written after the summer school in Trieste 2001. *Introduction of Modern Methods of Quantum Many-Body Theory and heir Applications*, Series on Advances in QUantum Many-Body Theory - VOl. 7, edited by A. Fabrocini, S. Fantoni and E. Krotscheck. A mandatory reading is the book by E. Feenberg, *Theory of Quantum Liquids,* [18] which contains the most complete monography on the variational theory applied to Quantum Liquids and that has enlightened most of the developments of the theory during the last forthy years.

1.1 General Properties of liquid helium

In order to get familiar with the energy and length scales associated to liquid helium, some of its general properties will be first reviewed. The helium atom has a very stable configuration that makes it chemically inert. Besides, its lowest excitation energy is around 20 eV and the ionization energy is 24.56 eV. These energies are quite high compared with the energy scales involve in the description of the liquid, which are of the order of few Kelvins (K) (notice that 1 eV equals 11604 K). For the same reasons, the polarizability of the He atom is very small, and as a consequence, the van der Waals interaction when two atoms are close together is rather small and translates into a weak attraction that nevertheless turns into a strong repulsion when the atoms overlap. The situation is such that one can forget about the internal structure of the atoms and consider them as the elementary constituents of the quantum liquid interacting through a two–body potential.

Actually this interaction is so weak that two ^{4}He atoms are very weakly bound, while two ^{3}He atoms are not bound at all. Notice also that the interaction between the atoms is due to the polarization of the electronic cloud, and as consequence the interaction between ^{4}He-^{4}He, ^{3}He-^{3}He, and ^{4}He-^{3}He pairs can be considered to be the same. Keeping this in mind, it is easy to understand that, being the ^{4}He-^{4}He system very weakly bound, the ^{3}He-^{3}He and ^{4}He-^{3}He systems, which have lighter mass but the same interaction, are not bound.

As it has been previously mentioned, both ^{4}He and ^{3}He remain liquid at zero temperature. It is commonly thought that cooling down a substance reduces the average kinetic energy of its atoms. If the temperature is decreased low enough, the atoms lose their mobility and get confined to fixed positions: at this point the substance solidifies. However, in this qualitative argument one is forgetting the uncertainty principle, which tells us that if the atoms are confined to a small region in space, then their momentum is not fixed, and so they acquire a non–zero average kinetic energy, the so called *zero point motion*.

One way to estimate this energy is to associate the volume occupied by each particle, $1/\rho$, to a spherical box, and to approximate the kinetic energy to the ground state energy of a particle moving in this spherical box $t \sim \hbar^2\pi^2/(2mR^2)$, R being its radius. At the saturation density of liquid ^{4}He, $\rho_0 = 0.0218$ Atoms/Å^3, one finds a volume of 46 Å^3, with $R = 2.22$ Å and $E \sim 12.3\,$K. This kinetic energy is large enough to compensate the interaction between the atoms that tries to locate them in fixed equilibrium positions, and that is the reason why helium remains liquid at $T = 0$. This is a macroscopic manifestation of quantum mechanics. The other noble gases are heavier and easier to polarize, and become solid at zero temperature. The phase diagram of liquid ^{4}He in the PT plane at low temperature is shown in Fig. 1. The line marked as λ–transition separates the normal (liquid He I) from the superfluid (Liquid He II) phases.

Several characteristic properties of ^{4}He and ^{3}He are reported in Table 1. Some of these properties can be qualitatively understood taking into account the different masses, the different statistics, and the fact that ^{4}He and ^{3}He have the

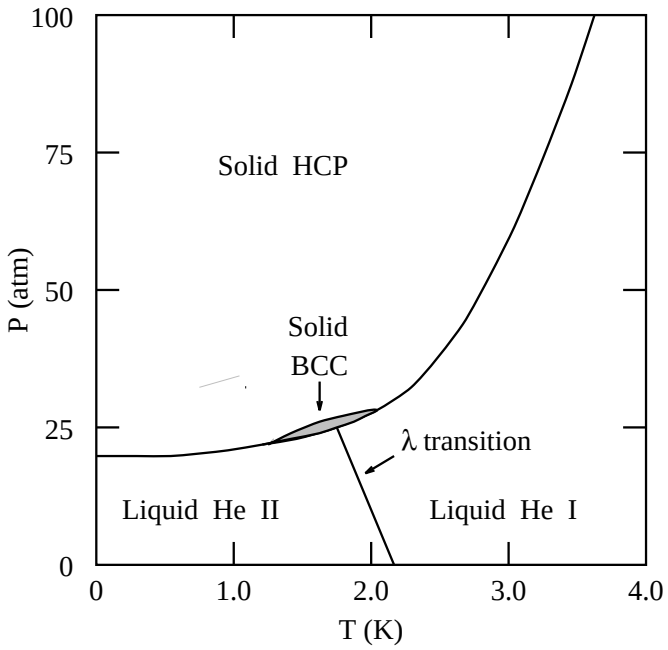

Figure 1: Schematic phase diagram of liquid ^{4}He in the PT plane.

same interaction. The lighter mass of ^{3}He atoms translates into a larger mobility and therefore into a smaller saturation density and smaller binding energy per particle. Notice also that the binding energy results from a strong cancellation between the potential and the kinetic energies. Actually, the value of the kinetic energy for liquid ^{4}He is a direct measure of the relevance of correlations. In the absence of interactions, the ground state has all the particles in the zero momentum state. When the interaction is turned on, particles are promoted out of the zero momentum state and the system ends up with a kinetic energy of about 14 K. However, there still remains a macroscopically large number of particles in the zero momentum state, that is measured by the condensate fraction value, $n_0 = N_0/N \neq 0$. At saturation density, the *condensate fraction* of liquid ^{4}He is of the order of 8%.

The volume per particle occupied by liquid ^{4}He is smaller than that of ^{3}He. Therefore, it is easier to compress liquid ^{3}He, and as a consequence the speed of sound in liquid ^{3}He is smaller than in liquid ^{4}He when they are compared at the corresponding saturation densities. When the interactions are turned off, the ^{3}He system is described by means of a Slater determinant of plane waves filling the *Fermi sphere or free Fermi sea*. The radius of the Fermi sphere is determined by the Fermi momentum which, at saturation density of liquid ^{3}He, corresponds to $k_F = 0.78$ Å^{-1}. The average kinetic energy per particle associated to the free Fermi sea is $e_F = 3\hbar^2 k_F^2/10m$ which is, at the same density, $e_F \sim 3K$. The

Table 1: Characteristic properties of helium liquids

	^{4}He	^{3}He
$\hbar^2/2m$	6.02 K Å^2	8.03 K Å^2
ρ_0	0.365 σ^{-3}	0.274 σ^{-3}
e_0	-7.17 K	-2.47 K
$\langle U \rangle$	$\sim$ -21 K	$\sim$ -15 K
$\langle T \rangle$	$\sim$ 14 K	$\sim$ 12 K
$1/\rho_0$	~ 46 Å^3	~ 61 Å^3
$V_{\rm atom} * \rho_0$	0.2	0.15
$v_{\rm sound}$	238 m/s	183 m/s
$P_{\rm sol}$	25 atm	34 atm

Fermi momentum defines the Fermi surface, a very important concept that is meaningful even for a normal Fermi liquid when the interactions are turned on.

Another quantity of interest is the binding energy of *one ^{3}He impurity* in liquid ^{4}He, $\mu = -2.78$ K at the ^{4}He saturation density. Notice that a ^{3}He impurity is more bound in liquid ^{4}He than the binding energy of liquid ^{3}He. This indicates that it is energetically more favorable to solve ^{3}He in ^{4}He than to have separate phases. As a consequence we have *stable liquid mixtures* of both isotopes, with a maximum solubility of $\sim 6\%$.

It is also worth noticing that the ratio of the volume occupied by each atom ($V_{atom} = 4\pi R^3/3$ with R$\sim$ 1.3 Å) to the volume it has at its disposal ($V = 1/\rho_0$) is approximately 0.2 for pure ^{4}He, thus indicating that the system is *highly packed* and that therefore the influence of correlations is strong. This same ratio for *nuclear matter* (an homogeneous system of nucleons that simulates matter at the center of a nucleus) would be 0.05. In this sense, liquid helium is more correlated than nuclear matter. From this point of view, convergence of perturbative calculations will be harder to achieve in liquid helium than in nuclear matter.

Finally, it is interesting to notice that in spite of the different scales in energy and length, from Kelvins to MeVs and from Angstroms to Fermis, the physics of both systems, liquid ^{3}He and nuclear matter, is similar. Also from the methodological point of view, and this is one of the strongest points of the many–body theory, one can use the same techniques to study them.

2 Microscopic description

The microscopic description of a quantum many–body system can be performed once the Hamiltonian, written in terms of the masses of the atoms and the interaction, is established

$$H \;=\; \sum_{i=1}^{N} \frac{p_i^2}{2m} \;+\; \sum_{i<j}^{N} V(r_{ij}) \;. \qquad (1)$$

In the following, only the description of infinite, homogeneous systems at $T = 0$ and in the thermodynamic limit ($N \to \infty$, $\Omega \to \infty$ but $\rho = N/\Omega \to$ *constant*) will be considered.

As the Hamiltonian is written in first quantization, the indistinguishability of particles is accounted in the *symmetry of the operators* entering in H. However, the Hamiltonian does not distinguish if the identical particles are bosons or fermions, and therefore this information should be added by hand to the *wave function*. As usual, the latter has to be even for a system of bosons and odd for a system of fermions under the exchange of any pair of particle coordinates.

The interaction depends only on the interparticle distance and a simple representation is the Lennard–Jones potential

$$V(r) = 4\epsilon \left[\left(\frac{\sigma}{r}\right)^{12} - \left(\frac{\sigma}{r}\right)^{6} \right], \tag{2}$$

where $\epsilon = 10.22$ K defines the depth of the potential and $\sigma = 2.556$ Å , the length scale.

Nowadays, one uses the more accurate Aziz (HFDHF2) potential [19]

$$V_{Aziz}(r) = \epsilon \left[A e^{-\alpha x} - F(x) \left(\frac{C_6}{x^6} + \frac{C_8}{x^8} + \frac{C_{10}}{x^{10}} \right) \right] , \tag{3}$$

where

$$F(x) = \begin{cases} \exp\left[-\left(\frac{D}{x} - 1\right)^2 \right] & x < D \\ 1 & x \geq D \end{cases} \tag{4}$$

and

$$x = \frac{r}{r_m} \tag{5}$$

with parameters

$$\begin{array}{ll} \epsilon = 10.8K & C_6 = 1.3732412 \\ r_m = 2.9673\,\text{Å} & C_8 = 0.4253785 \\ D = 1.241314 & C_{10} = 0.1781 \\ \alpha = 13.353384 & A = 5.448504 \cdot 10^5 \ , \end{array} \tag{6}$$

and its revised version HFD-B(HE), [20] are used in realistic calculations.

The He-He potential is characterized by a strong short range repulsion (such that in a first approximation, the atoms can be considered as hard spheres of diameter $\sim 2.6\,$Å) and a weak attraction at medium and large distances. The Lennard–Jones and the Aziz potential are compared in Fig. 2. Despite the apparent similarities, $V_{Aziz}(r)$ appreciably differs from $V_{LJ}(r)$ at short distances where in particular the former does not diverge. In this sense, $V_{Aziz}(r)$ has a softer core.

To solve the many–body Schrödinger equation is not an easy task and only in very few exceptional cases one is able to find an exact analytic solution. In

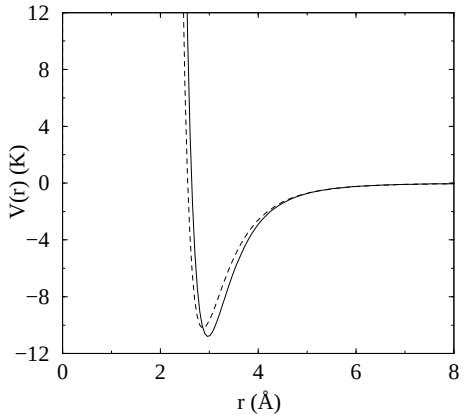

Figure 2: Comparison between the Lennard–Jones (dashed–line) and the Aziz (solid line) potentials.

addition, the *presence of the hard core* in the interaction makes the application of standard perturbative methods difficult. This is because the matrix elements entering in the perturbative series would be too large, and also due to the fact that these are very dense systems. An efficient way to handle the short range correlations induced by the core of the potential is to embed them, from the very beginning, in a trial wave function Ψ_T describing the system with N atoms

$$\Psi_T(1,\ldots,N) = F(1,\ldots,N)\phi(1,\ldots,N) \ . \tag{7}$$

The correlation operator factor F, which is symmetrical with respect to the exchange of particles, incorporates to the wave function in a direct but approximate way the dynamic correlations induced by the interaction between the atoms. $\phi(1,\ldots,N)$ is the wave function corresponding to the free gas, which describes the system when the interactions are turned off and keeps the correct symmetry of the total wave function.

For the ground state, one usually places all particles in the zero momentum state and so $\phi(1,\ldots,N) = \Omega^{-N/2}$. For fermions, the model function $\phi(1,\ldots,N)$ is chosen as the Slater determinant associated to the free Fermi sea

$$\phi(1,\ldots,N) = det \mid \psi_{\alpha_i}(j) \mid . \tag{8}$$

The single–particle wave functions $\psi_{\alpha_i}(j)$, where the subscript refers to the state, are taken as plane waves

$$\psi_{\alpha_i}(j) = \frac{1}{\Omega^{1/2}} e^{i\mathbf{k}_{\alpha_i}\cdot\mathbf{r}_j}\sigma(j) \ , \tag{9}$$

$\sigma(j)$ representing the spin contribution. In the ^{3}He case, $\sigma(j)$ refers to the third component of the spin and so it can be either $\mid +\rangle$ or $\mid -\rangle$. In this way, each momentum state has a degeneracy 2.

These plane waves satisfy the boundary conditions in a large cube of volume Ω which becomes infinite when the thermodynamic limit is considered. The allowed momenta fill a Fermi sphere of radius $k_F = (6\pi^2\rho/\nu)^{1/3}$, where $\nu = 2$ is the spin degeneracy. Once a trial wave function is defined, the variational principle guarantees that the expectation value of the Hamiltonian

$$\frac{\langle \Psi_T \mid H \mid \Psi_T \rangle}{\langle \Psi_T \mid \Psi_T \rangle} = E_T, \tag{10}$$

is an upper bound to the ground state energy E_0. Obviously, for the method to be efficient, the trial wave function must yield a *good representation* of the real many–body ground state wave function. Simple as it may look, the evaluation of the expectation value is by no means an easy task, and very sophisticated algorithms requiring large computer capabilities have been devised during the last years. [12]

In this way, the ingredients for a variational calculation are the Hamiltonian and the wave function. In addition, one needs a powerful and efficient machinery to *evaluate the expectation values*. At this point, one should appeal to the physical intuition in order to choose an appropriate trial wave function describing the system under consideration. A good starting point is to use a *Jastrow correlation operator* [21]

$$F(1,...,N) = F_2(1,...,N) = \prod_{i<j} f_2(r_{ij}) \ , \tag{11}$$

$f_2(r)$ being a properly chosen two–body correlation function that should be zero or almost zero when the interparticle distance is smaller than the range of the repulsive part of the potential that characterizes the interaction between the atoms, it should go to unity at large distances manifesting the absence of correlations when particles are separated far away from each other.

One way to proceed is to use a correlation function with an analytical expression depending on several free parameters, whose values are chosen to minimize the total energy. In this way, one determines the best function within the functional space defined by the variation of these parameters. Another alternative that will be discussed later on is to *solve the Euler–Lagrange equations* associated to the problem

$$\frac{\delta}{\delta f_2} \frac{\langle \Psi_T \mid H \mid \Psi_T \rangle}{\langle \Psi_T \mid \Psi_T \rangle} = 0 \tag{12}$$

which yields the optimum correlation factors. Before discussing the determination of the optimum two–body correlation factor, one must find a good and efficient way to evaluate the expectation value of the Hamiltonian.

On top of that one has to perform a *cluster expansion* of the multidimensional integrals involved in the evaluation of the expectation value of the energy and to try a systematic summation of the different terms.

Another possibility is to use *Monte Carlo methods*, based on the Metropolis algorithm, to evaluate the multidimensional integrals appearing in the expressions of E_T, and this particular application is known as variational Monte Carlo

method (VMC). One important thing to keep in mind is that, apart from finite size effects associated to the fact that the Monte Carlo calculation takes place in a finite box with a finite number of particles, Monte Carlo provides an exact result for that given trial wave function and can be used as an accuracy check for the calculations described here.

Other more powerfull Monte Carlo methods like diffusion Monte Carlo and path integral ground state Monte Carlo methods have been developed recently. These methods would be a subject of a separate course.

Let us begin by introducing *the concept of a distribution function*, which appear in a natural way in the evaluation of the expectation value of a many–body Hamiltonian. The *calculation of the expectation value of the potential energy* per particle can be carried out as follows. The indistinguishability of particles is reflected in the potential operator, which is symmetric under the exchange of coordinates, and in the wave function, which is symmetric for bosons and antisymmetric for fermions. Therefore, any pair of particles contributes the same to the potential energy, which then becomes

$$\begin{aligned}\frac{1}{N}\langle V\rangle &\equiv \frac{1}{N}\frac{\langle\Psi_T \mid \sum_{i<j} V(r_{ij}) \mid \Psi_T\rangle}{\langle\Psi_T \mid \Psi_T\rangle} \\ &= \frac{N(N-1)}{2}\frac{1}{N}\frac{\langle\Psi_T \mid V(r_{ij}) \mid \Psi_T\rangle}{\langle\Psi_T \mid \Psi_T\rangle} \ .\end{aligned}$$

where $r_{ij} = |\mathbf{r}_i - \mathbf{r}_j|$, and the potential is independent of angles.

After that, one can carry out the integrals over coordinates $\mathbf{r}_3, \ldots, \mathbf{r}_N$ and write

$$\frac{1}{N}\langle V\rangle = \frac{1}{N}\frac{1}{2}\rho^2 \int d\mathbf{r}_1 d\mathbf{r}_2 V(r_{12}) g(r_{12}) \tag{13}$$

where $g(r)$ is the two–body radial distribution function

$$g(r) = \frac{N(N-1)}{\rho^2}\frac{\int \mid \Psi_T(1,\ldots,N) \mid^2 d\mathbf{r}_3 \cdots d\mathbf{r}_N}{\int \mid \Psi_T(1,\ldots,N) \mid^2 d\mathbf{r}_1 \cdots d\mathbf{r}_N} \ . \tag{14}$$

For uniform and homogeneous systems, $g(r)$ depends only on the magnitude of $\mathbf{r}$ and is proportional to the probability of finding two particles separated by a given distance r, normalized such that $g(r) \to 1$ when $r \to \infty$. Therefore, changing from variables $(\mathbf{r}_1, \mathbf{r}_2)$ to $(\mathbf{r}_1, \mathbf{r} = \mathbf{r}_2 - \mathbf{r}_1)$, and performing the trivial integration over $\mathbf{r}_1$, one finds

$$\frac{1}{N}\langle V\rangle = \frac{1}{2}\rho \int d\mathbf{r}\, V(r) g(r) \ , \tag{15}$$

and thus the calculation of the potential energy is translated into the calculation of the distribution function $g(r)$.

Similar things happen with the evaluation of the *kinetic energy*. In order to illustrate how it can be calculated, the simple case of a bosonic system described through a Jastrow wave function will be considered. Again and due to the

indistinguishability of particles reflected in the symmetry of the wave function, all terms contribute the same and one has

$$\frac{1}{N}\langle T\rangle = -\frac{1}{N}\sum_{i=1}^{N}\frac{\hbar^2}{2m}\frac{\langle\Psi_T \mid \sum\nabla_i^2 \mid \Psi_T\rangle}{\langle\Psi_T \mid \Psi_T\rangle} \equiv -\frac{\hbar^2}{2m}\frac{\langle\Psi_T \mid \nabla_1^2 \mid \Psi_T\rangle}{\langle\Psi_T \mid \Psi_T\rangle} \ . \tag{16}$$

For the real wave function the kinetic energy part of the Hamiltonian can be written as

$$\frac{\hbar^2}{2m}\Psi_T\nabla_1^2\Psi_T = \frac{\hbar^2}{8m}\nabla_1^2\Psi_T^2 + \frac{\hbar^2}{8m}\Psi_T^2\nabla_1^2\log(\Psi_T^2) \tag{17}$$

The expectation value of the first term vanishes because we can use Gauss' law of integration and assume that the derivative of the wave function vanishes at the infinity.

Identifying the expression of the distribution function, and performing the same change of variables done in the evaluation of the potential energy, one finally finds

$$\frac{1}{N}\langle T\rangle_{JF} = \frac{1}{2}\rho\frac{\hbar^2}{2m}\int d\mathbf{r}g(r)(-\nabla^2\ln f_2(r)) \ . \tag{18}$$

Notice that even if T is a one–body operator, the presence of two–body correlations in the wave function makes its expectation value depend on the two–body radial distribution function $g(r)$.

Collecting results (15) and (18), one finally arrives at the expression of the total energy of a boson fluid described by a Jastrow wave function

$$\frac{1}{N}\frac{\langle\Psi_T \mid H \mid \Psi_T\rangle}{\langle\Psi_T \mid \Psi_T\rangle} = \\ = \frac{1}{2}\rho\int d\mathbf{r}g(r)\left[V(r) - \frac{\hbar^2}{2m}\nabla^2\ln f(r)\right] \ . \tag{19}$$

The angular integration can be trivially performed, and therefore if $g(r)$ is known, the evaluation of the energy reduces to a one dimensional quadrature. Thus the whole problem has been translated into the evaluation of the two–body radial distribution function.

A rather simple $f_2(r)$ which has been extensively used in the study of ^{4}He and ^{3}He liquids is the so called McMillan or Schiff–Verlet correlation factor [25, 26]

$$f_2(r) = \exp\left[-\frac{1}{2}\left(\frac{b\sigma}{r}\right)^5\right] \ . \tag{20}$$

This function approximates well the short range behavior of the optimal correlation factor, and approaches quickly to unity. Besides, it is basically zero inside the core of the potential. The energy is minimized with respect to b, which is taken as a variational parameter.

2.1 General properties of the ground state

Before concentrating on the calculation of the *optimal distribution function*, it is useful to discuss a couple of *general properties* of the ground state wave function of a bosonic system, because they serve as a guide to write a *general ansatz* for the variational many–body wave function. In a boson system the wave funtion has two important properties:

1. It has no nodes, that is, it does not change sign and so can be chosen real and positive.

2. is not degenerate.

The proof begins by writing the ground state wave function of the many–body boson systems in a general exponential form [27]

$$\Psi_0(\mathbf{r}_1, \ldots, \mathbf{r}_N) = \exp\left[\frac{1}{2}\chi(\mathbf{r}_1, \ldots, \mathbf{r}_N)\right] , \tag{21}$$

where χ is a complex function

$$\chi(\mathbf{r}_1, \ldots, \mathbf{r}_N) = \chi_R(\mathbf{r}_1, \ldots, \mathbf{r}_N) + \imath\chi_I(\mathbf{r}_1, \ldots, \mathbf{r}_N) \tag{22}$$

with χ_R and χ_I real and symmetric under the exchange of particle coordinates. Note that this form is general enough to represent the ground state, allowing for the presence of nodes in Ψ_0.

The first thing to realize is that the expectation value of the potential energy does not depend on χ_I

$$\begin{aligned}\langle V\rangle &= \frac{\langle\Psi_0 \mid \sum_{i<j}^N V(r_{ij}) \mid \Psi_0\rangle}{\langle\Psi_0 \mid \Psi_0\rangle} \\ &= \frac{\int d\mathbf{r}_1 ... d\mathbf{r}_N \sum_{i<j}^N V(r_{ij}) \exp[\chi_R(\mathbf{r}_1, ..., \mathbf{r}_N)]}{\int d\mathbf{r}_1 ... d\mathbf{r}_N \exp[\chi_R(\mathbf{r}_1 ..., \mathbf{r}_N)]}\end{aligned}$$

while, on the other hand, and using the Jackson–Feenberg identity , the kinetic energy can be written as

$$\begin{aligned}\langle T\rangle &= \frac{\langle\Psi_0 \mid \frac{-\hbar^2}{2m}\sum_{i=1}^N \nabla_i^2 \mid \Psi_0\rangle}{\langle\Psi_0 \mid \Psi_0\rangle} \\ &= \frac{\int d\mathbf{r}_1 ... d\mathbf{r}_N\, e^{\chi_R}\left[-\frac{\hbar^2}{8m}\sum_{i=1}^N (\nabla_i^2\chi_R) + \frac{\hbar^2}{8m}\sum_{i=1}^N (\nabla_i\chi_I)^2\right]}{\int d\mathbf{r}_1 ... d\mathbf{r}_N \exp[\chi_R]} .\end{aligned}$$

The kinetic energy splits in two pieces, the second one depending on χ_I and being positive definite. As a consequence, one can always decrease the energy by setting $\chi_I = 0$. But if $\chi_I = 0$, then it is clear that the wave function has no nodes, is real and does not change sign. The fact that Ψ_0 is non–degenerate is a consequence of the absence of nodes. If there was another eigenstate with

the same energy, it would be possible to take it orthogonal to Ψ_0. However, in order to be orthogonal to Ψ_0, this new eigenstate would have to show at least one node, and therefore $\chi_I(\mathbf{r}_1, ..., \mathbf{r}_N) \neq 0$. But then it would be possible to lower once again the energy of that state by choosing $\chi_I = 0$, contradicting the hypothesis that E_0 was the lowest possible energy. This can not happen and therefore Ψ_0 is non–degenerate.

In conclusion, the ground state wave function of a Bose system can be written in the form

$$\Psi_0(\mathbf{r}_1, \ldots, \mathbf{r}_N) = \exp\left[\frac{1}{2}\chi_R(\mathbf{r}_1, \ldots, \mathbf{r}_N)\right] \ , \tag{23}$$

where the function χ_R can be decomposed into n–body functions u_n, with $1 \leq n \leq N$

$$\chi_R(\mathbf{r}_1, \ldots, \mathbf{r}_N) = \sum_{n=1}^{N} \sum_{i_1, \ldots, i_n} u_n(\mathbf{r}_{i_1}, \ldots, \mathbf{r}_{i_n}) \ , \tag{24}$$

with the summation on $i_1 \ldots i_n$ running over all possible choices of n indices from the set $(1, \ldots, N)$. More explicitly

$$\begin{aligned} \Psi_0(\mathbf{r}_1, \ldots, \mathbf{r}_N) = \exp\Big[&\frac{1}{2}\sum_{i<j}^{N} u_2(r_{ij}) \\ &+ \frac{1}{2}\sum_{i<j<k} u_3(\mathbf{r}_i, \mathbf{r}_j, \mathbf{r}_k) + \cdots\Big] \end{aligned} \tag{25}$$

which is known as the *Feenberg ansatz*.

An equivalent way to write this wave function would be

$$\Psi_0(\mathbf{r}_1, \ldots, \mathbf{r}_N) = \prod_{i<j} f_2(r_{ij}) \prod_{i<j<k} f_3(\mathbf{r}_i, \mathbf{r}_j, \mathbf{r}_k) \ldots \ . \tag{26}$$

with $f_n = e^{u_n/2}$.

In this way, the *Jastrow wave function* containing only two body correlations

$$\Psi_J(\mathbf{r}_1, \ldots, \mathbf{r}_N) = \prod_{i<j} f_2(r_{ij}) = e^{\frac{1}{2}\sum_{i<j}^{N} u_2(r_{ij})} \tag{27}$$

can be considered as the first step towards a systematic approach to the exact ground state wave function of a boson fluid.

The previous expressions serve to identify the *general structure of the wave function*, but do not provide enough information to determine the correlation functions entering. One knows from basic grounds, however, that there are general requirements they should fulfill

- They should be real functions in order to yield a real total wave function.
- They must be symmetric under the exchange of particle coordinates.

- They must be invariant under translation of the center of mass of the particles involved in the correlation

$$\mathbf{R} = \frac{1}{n}\sum_{i=1}^{n} \mathbf{r}_i \ . \tag{28}$$

- They have to be invariant under rigid rotations around the center of mass $\mathbf{R}$.
- They have to be invariant under simultaneous inversion of all the coordinates.
- They should fulfill the cluster property, which means that $u_n(\mathbf{r}_1, \ldots, \mathbf{r}_N)$ has to vanish whenever any one of the coordinates becomes arbitrarily large.

Particularly, the cluster condition implies that the decomposition of χ_R given in Eq. (25) is unique.

All those conditions must be also fulfilled when the correlation operator is expressed in terms of $F(1, \ldots, N)$. In fact, if any subset, $i_1, \ldots i_p$, of particles is separated from the rest, $F(1, \ldots, N)$ decomposes in a product of two factors

$$F(1, \ldots, N) = F_p(i_1, \ldots, i_p) F_{N-p}(i_{p+1}, \ldots, i_N) \ . \tag{29}$$

Finally, notice that the cluster property particularly implies that

$$f^{(2)}(r \to \infty) \to 1 \ , \tag{30}$$

and that all the previous properties apply equally well in the case when one uses an approximate wave function of the Jastrow type with two–body correlation factors only.

3 Hypernetted–chain equations

It has been shown in the previous section that the energy per particle of an homogeneous bosonic system can be easily calculated once the two–body radial distribution function $g(r)$ is known. In this sense, $g(r)$ is the key quantity required in most variational calculations. The main goal of this section is to learn how it can be calculated. For a Jastrow wave function, $g(r)$ becomes

$$g(r) = \frac{N(N-1)}{\rho^2} \frac{\int \prod_{i<j} f_2^2(r_{ij})\, d\mathbf{R}_{12}}{\int \prod_{i<j} f_2^2(r_{ij})\, d\mathbf{R}} \ . \tag{31}$$

where $d\mathbf{R}_{12} = d\mathbf{r}_3 d\mathbf{r}_4 \ldots \mathbf{r}_N$ and $d\mathbf{R} = d\mathbf{r}_1 d\mathbf{r}_2 \ldots \mathbf{r}_N$

In order to calculate $g(r)$ it is useful to introduce the *cluster* function $h(r) = f_2^2(r) - 1$. Because of the healing property of $f_2(r)$ that makes it approach unity when the distance increases, the function $h(r)$ goes quickly to zero and provides a plausible expansion parameter. In fact, both the numerator and the denominator of Eq. (31) can be expanded in powers of the function $h(r)$

$$g(r) = \frac{N(N-1)\Omega^{-N}}{\rho^2\Omega^{-N}} \times \tag{32}$$
$$\times \frac{\int d\mathbf{R}_{12} \left(1 + \sum_{i<j} h(r_{ij}) + \sum_{i<j,k<l} h(r_{ij})h(r_{kl}) \dots\right)}{\int d\mathbf{R} \left(1 + \sum_{i<j} h(r_{ij}) + \sum_{i<j,k<l} h(r_{ij})h(r_{kl}) \dots\right)}$$

where a factor Ω^{-N} corresponding to the normalization of the non–interacting wave function has been added both in the numerator and the denominator. The resulting contributions become multidimensional integrals involving one or more $h(r)$ factors, which are referred to as *cluster terms*. Doing so leads to an expression that apparently looks much worse than the original one, but that is easier to deal with as it will be shown in the following.

Two important facts allowing for enormous simplifications should be taken into account:

- many integrals give the same result,
- there are substantial cancellations between infinite sets of terms.

The best way to understand how to take advantage of these facts is, as in many branches of modern physics, by introducing a diagrammatic notation.

Cluster diagrams are built with dashed lines representing functions $h(r_{ij})$ connecting particles i and j, and points or circles denoting the particles themselves. In order to get used to this diagrammatic notation, Fig. 3 shows some of the diagrammatic contributions resulting from the cluster expansion of the numerator. Particles 1 and 2, which are not integrated, appear as open circles in the diagrams. On the other hand, internal points corresponding to integrated coordinates are represented by solid circles. Many different terms, as for example $\int d\mathbf{r}_3 h(r_{13})h(r_{23})$ and $\int d\mathbf{r}_7 h(r_{17})h(r_{27})$, yield the same value since internal points are nothing but dummy integration variables. They are represented by the same diagrammatic structure but with different labeling of the internal points. In this way, it is clear that disregarding the labeling, a given diagram corresponds to many different cluster integrals. In the diagrammatic formalism, all these terms are represented by a single unlabeled diagram multiplied by a properly chosen weighting factor that takes this fact into account.

Weighting factors are built from combinations of three different quantities: first, terms of the form $(N - \alpha)$ which have to do with the different ways in which internal points can be drawn from a set of $N - 2$ particles (corresponding to the total number of particles N minus the two external points that are fixed); second, factors Ω resulting from the cancellation of the global $1/\Omega^N$ term (Eq. (33)) and the integral over the coordinates not appearing in the diagram;

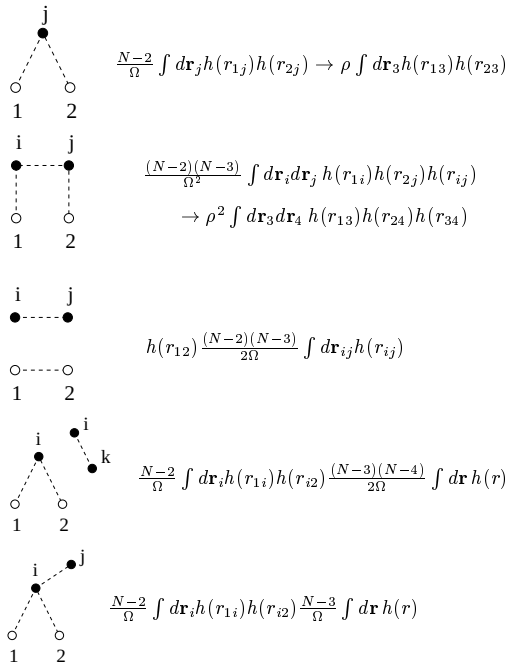

Figure 3: Several cluster diagrams appearing in the numerator of Eq. (33)

and third, overall symmetry factors associated to the fact that sometimes permutations of the labels corresponding to internal points in a given diagram leads to exactly the same labeled diagram. All this is summarized in Fig. 3, where it is also indicated how in the thermodynamic limit factors of the form $(N-\alpha)/\Omega$ turn into densities ρ.

As an example, the third diagram has a function $h(r_{12})$ multiplying because neither coordinate 1 nor 2 are being integrated. It also contains a factor $(N-2)(N-3)$ corresponding to choosing two points (i and j in the diagram) from $N-2$ possible choices. There is also an overall Ω dividing, that results from the cancellation of the $1/\Omega^N$, and a factor Ω^{N-4} from the integration over all the remaining particle coordinates (different from 1, 2, i and j), a factor Ω from the change of variables $\int d\mathbf{r}_1 d\mathbf{r}_2 \to \int d\mathbf{R} d\mathbf{r} = \Omega \int d\mathbf{r}$ with $\mathbf{R} = (\mathbf{r}_1 + \mathbf{r}_2)/2$ and $\mathbf{r} = \mathbf{r}_1 - \mathbf{r}_2$ and a factor Ω^2 coming from the ρ^2 in the definition of $g(r)$. And finally, a symmetry factor $1/2$ associated to the fact that exchanging the labels i and j leads to exactly the same diagram. All other diagrams in the figure can be analyzed in the same way.

Furthermore and as mentioned above, there are strong cancellations between diagrams in the numerator and the denominator of $g(r)$. These cancellations can be identified once the different cluster integrals are properly classified. Since integrals are represented by diagrams, the problem of classifying the cluster

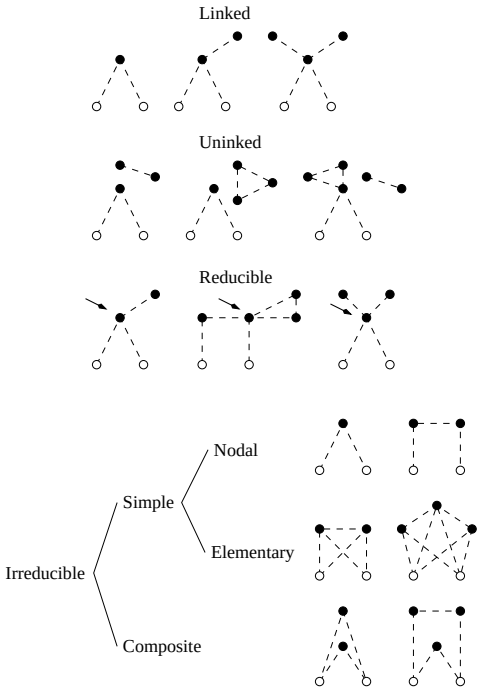

Figure 4: Classification of cluster diagrams

integrals is directly mapped into the problem of classifying diagrams.

The standard classification of diagrams is illustrated in Fig. 4. Reduced to its fundamental topological essence, diagrams may be *linked and unlinked*. Unlinked diagrams contain separated pieces not connected to each other by correlation lines. In contrast, linked diagrams form one single piece and therefore one can always find at least one path of lines connecting any pair of points in the diagram. Examples of linked and unlinked diagrams are depicted in the first two rows of Fig. 4.

Linked diagrams can be classified as *reducible* and *irreducible*. Reducible diagrams are those with at least one *articulation point*. An articulation point is a circle separating the diagram in two or more different parts, such that any path of lines joining one particle in one part to another particle in another part passes always through it. Furthermore, all the external points in a reducible diagram remain in the same part.

Examples of reducible diagrams are also shown in Fig. 4, pointing with an arrow the articulation points. Due to the translational invariance of $h(r)$, the integral expression associated with a reducible diagram can always be factorized into independent pieces. Despite the apparent simplicity of the classification, it is still difficult to decide which diagrams are relevant in the evaluation of $g(r)$.

Fortunately, there is a useful theorem that simplifies the situation a lot.

This *linked cluster theorem states that one needs to consider only the irreducible diagrams of the numerator.* All unlinked and reducible diagrams cancel against the denominator of Eq. (33) up to order 1/N. A somewhat elaborated proof of the theorem, as an special application of the more general fermionic case, has been given by Fantoni and Rosati. [29] On the other hand, this problem is completely equivalent to the calculation of the radial distribution function of a classical fluid at finite temperature

$$g(r) = \frac{N(N-1)}{\rho^2} \frac{\int d\mathbf{R}_{12} \exp\left[-\sum V(r_{ij})/kT\right]}{\int d\mathbf{R} \exp\left[-\sum V(r_{ij})/kT\right]}, \tag{33}$$

where k is Boltzmann's constant. The parallelism is established by identifying, $f_2(r_{ij})$ with $\exp[-V(r_{ij})/2kT]$. Therefore, one can use the experience accumulated in this field, [30] for which a diagrammatic notation was also introduced, and derive a Hypernetted–Chain (HNC) equation in a similar way as Leeuwen, Groeneveld and de Boer did for classical systems. [31]

In any case, one still has to face the problem of adding up the *contribution of all the irreducible diagrams in the numerator.* To this end, one needs to dive a little bit more into diagrammatic concepts and introduce new definitions. Irreducible diagrams can be classified as either *simple.* or *composite.* A simple diagram is a diagram containing only one $1-2$ *subdiagram*, while a composite diagram contains two or more $1-2$ *subdiagrams.* An $i-j$ *subdiagram* is a part of a diagram connected to the rest of the diagram through points i and j only. In particular, the first two diagrams in Fig. 3 are examples of diagrams with only one $1-2$ *subdiagram.*

Besides, simple diagrams can be divided in *nodal* and *elementary.* A *nodal* diagram is a diagram that has at least one *node.* A *node* is a point of the diagram, such that all paths of lines going from one external point to the other passes through it. An elementary diagram is a simple diagram that is non–nodal. In Fig. 4 there is a scheme showing the complete classification of diagrams. The final diagrammatic rules are very simple: diagrams are built with correlation lines and points. External points, representing particle coordinates 1 and 2, are depicted as open circles, while internal points (solid circles) imply an integration over the corresponding coordinates times a factor ρ. The sum of all topologically distinct irreducible diagrams defines the radial distribution function $g(r)$.

There are two mathematical operations associated to the construction of diagrams (see Fig. 5): the convolution and the algebraic products. The convolution product of two generic functions $a(r_{ik})$ and $b(r_{kj})$ representing diagrammatic links between points i and k and k and j respectively

$$\rho(a(r_{ik}) \mid b(r_{kj})) \equiv \rho \int d\mathbf{r}_k a(r_{ik}) b(r_{kj}) \ , \tag{34}$$

generates a nodal $i-j$ subdiagram that has point k as a nodal point. This is easy to understand since once the integral is performed, point k becomes an internal point that is the only link connecting the external point i in $a(r_{ik})$ to the external point j in $b(r_{kj})$, thus being a node. On the other hand, the

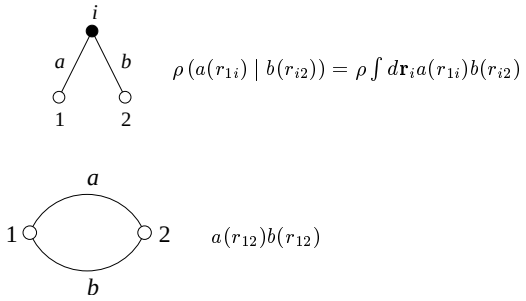

Figure 5: Mathematical operations associated to the construction of nodal and composite diagrams

algebraic product of two functions $a(r_{ij})$ and $b(r_{ij})$, which can be taken as two $i-j$ subdiagrams, generates a composite $i-j$ subdiagram.

At this point one is ready to derive the HNC equation in its simplest form, adding the contribution of all diagrams except those containing elementary pieces, which will be discussed later. The first row of Fig. 6 shows the diagrammatic contents of the chain equation at the first level of iteration. Let $N(r)$ be the sum of all the nodal diagrams, and take only, for the sake of simplicity, the subset of nodal diagrams resulting from the first iteration of the chain equations, as illustrated in the upper part of Fig. 6. If now one performs the convolution product of $N(r)$ and $h(r)$, which is the basic brick used to construct the chain, one gets all the diagrams of $N(r)$ except the first one which is the convolution product of two $h(r)$ function, as it is shown in the lower part of Fig. 6. The chosen set of diagrams satisfy therefore the equation

$$\rho(h(r_{1j}) \mid N(r_{j2})) = N(r_{12}) - \rho(h(r_{1j}) \mid h(r_{j2}))\ . \tag{35}$$

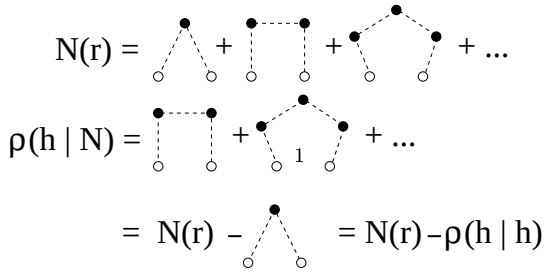

Figure 6: Diagrammatic scheme of the chain operation connecting diagrams.

The function $N(r)$ built in this way can then be used to construct composite diagrams. Composite diagrams have two or more $1-2$ subdiagrams, and so their sum has to be built from terms of the form $N^2(r), N^3(r), \ldots$ producing composite diagrams with $2, 3$ or more $1-2$ subdiagrams. However, these contributions must include appropriate symmetry factors in order to avoid undesired overcountings. As for example, $N^2(r)$ is the product of a sum of nodal diagrams with itself, thus producing diagonal terms squared and cross terms multiplied by 2. In the diagrammatic formalism, diagonal terms squared have to be divided by 2, which is the right symmetry factor correcting the fact that exchanging all particles in one of the subdiagrams with all particles in the other leads to exactly the same composite diagram. On the other hand, the factor 2 in the cross terms has to be removed as the previous situation does not happen here. Both facts are properly taken into account by replacing $N^2(r)$ with $N^2(r)/2!$.

Similar analysis leads to the conclusion that composite diagrams containing three $1-2$ subdiagrams have to be built from the combination $N^3(r)/3!$, and so on. The total sum of composite diagrams formed in this way becomes

$$\begin{aligned} N^2(r)/2! + N^3(r)/3! + N^4(r)/4! + \cdots \\ = \exp[N(r)] - N(r) - 1 \end{aligned} \tag{36}$$

in the thermodynamic limit. This is schematically shown in Fig. 7, where the diagrammatic contents of the exponential is explicitly depicted.

Finally, it should be noticed that one can still build new composite diagrams by multiplying $\exp[N(r)]$ with $h(r)$, thus producing the same composite diagrams but with an extra correlation line connecting external points 1 and 2. Since both $\exp[N(r)]$ and $h(r)\exp[N(r)]$ are possible, and $1+h(r) \equiv f_2^2(r)$, one finally finds the total sum of composite diagrams $X(r)$ to be

$$X(r) = f_2^2(r)\exp(N(r)) - N(r) - 1 \ . \tag{37}$$

$X(r)$ and $N(r)$ obtained through Eqs. (35) and (37) are the result of the first iteration in the HNC scheme. One can then use this $X(r)$ back as the building block of the chain and obtain $N(r)$ in the second iteration

$$\rho(X(r_{1j}) \mid N(r_{j2})) = N(r_{12}) - \rho(X(r_{1j}) \mid X(r_{j2})) \ , \tag{38}$$

and use this new nodal function in Eq. (37) to obtain $X(r)$ in the second iteration. This process must be repeated until convergence is reached. At that point, $X(r)$ and $N(r)$ simultaneously satisfy Eqs. (35) and (37), which constitute the set of HNC equations.

This scheme is commonly known as HNC/0, and its solution yields the sum of all diagrams but those containing elementary contributions. Elementary diagrams can be incorporated to the HNC process by including them in the definition of $X(r)$

$$X(r) = f_2^2(r)\exp\left[N(r) + E(r)\right] - N(r) - 1 \ , \tag{39}$$

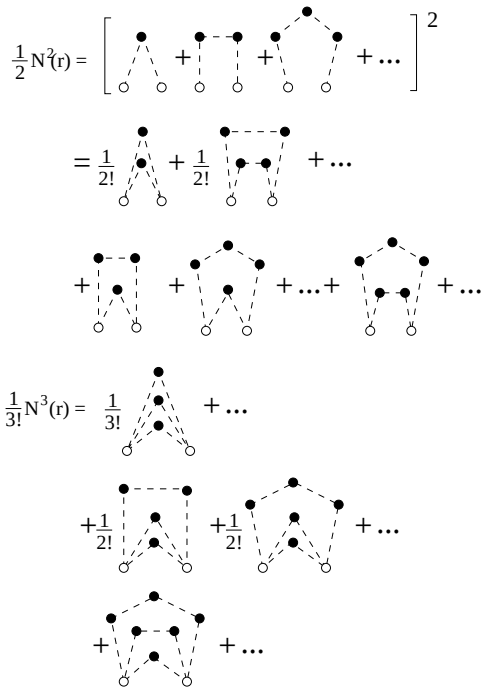

Figure 7: Diagrammatic contents of $\exp[N(r)]$.

although they can not be treated in an exact way because there are not simple relations connecting them to $N(r)$ or $X(r)$ in a closed form.

In the end, the *distribution function* is expressed as the sum of all nodal, composite and elementary diagrams

$$g(r) = 1 + X(r) + N(r) = f_2^2(r) \exp[N(r) + E(r)] \ . \tag{40}$$

The HNC equations (Eq. (38) and (39)) form a non linear set of integral equations, whose solution suggests in a natural way the iterative process discussed above that is illustrated in the scheme shown in Fig. 8.

Notice also that while doing the iterations, one can take advantage of the known properties of the Fourier Transform (FT), which turns convolutions into algebraic products and thus helps for solving at each step the nodal contributions from Eq. (38)

$$\tilde{N}(k) = \frac{\tilde{X}^2(k)}{1 - \tilde{X}(k)} \ , \tag{41}$$

where it is customary to define the FT in the HNC context as

$$\tilde{a}(k) = \rho \int d\mathbf{r}\, e^{i\mathbf{k}\cdot\mathbf{r}} a(r) \ , \tag{42}$$

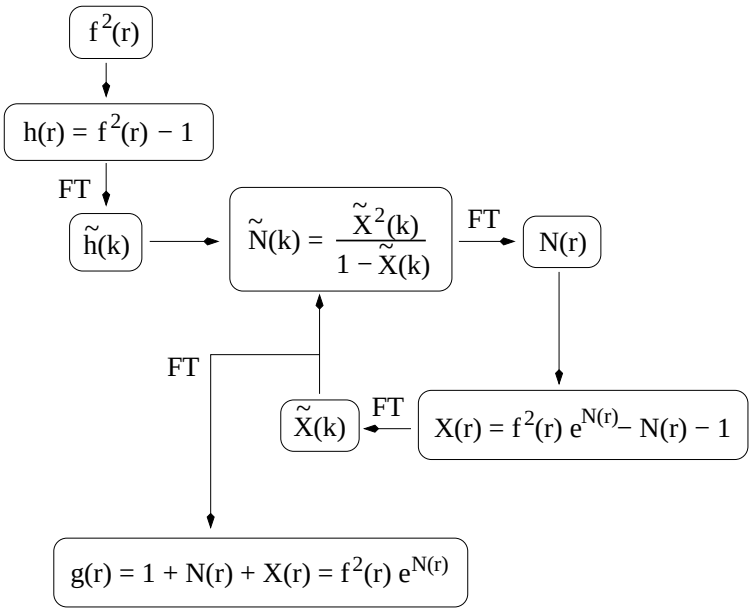

Figure 8: Iterative scheme to solve the HNC equations

including a density factor ρ.

According to the scheme in the figure, in the iterative process one usually calculates $X(r)$ (sum of composite and elementary diagrams) in r space and the nodal function in k space. In order to do so, good FT subroutines able to accurately treat correlations inside the core of the potential are required. Alternatively, the whole process can be carried out in position space, although convolutions may be harder to deal with. Usually, ten to twenty iterations are enough to reach convergence, at least for correlation factors with no long range order. Since each iteration is built from the results obtained in the previous one, the number of diagrams included at each steps grows exponentially.

One function which is experimentally accessible is the static structure function, defined as the Fourier transform of the radial distribution function

$$S(k) \equiv 1 + \rho \int d\mathbf{r}\, e^{i\mathbf{k}\cdot\mathbf{r}} (g(r) - 1) = 1 + \tilde{X}(k) + \tilde{N}(k) \ . \tag{43}$$

Taking into account the HNC equation, the nodal and the composite diagrams can be expressed in terms of the static structure function as

$$\tilde{N}(k) = \frac{(S(k) - 1)^2}{S(k)} \tag{44}$$

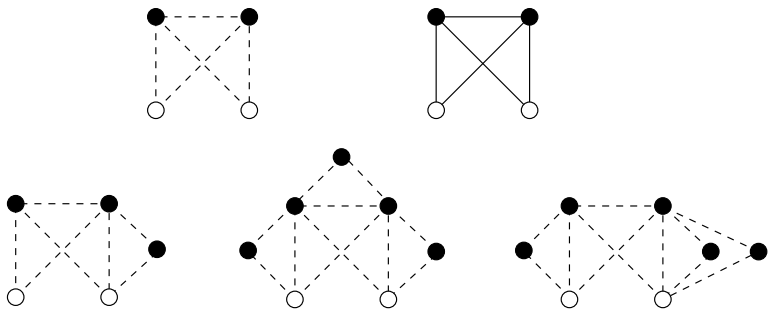

Figure 9: Four–points elementary diagrams and other elementary diagrams with the same basic structure. Dashed and solid lines represent factors $h(r)$ and $g(r)-1$, respectively.

and

$$\tilde{X}(k) = \frac{S(k)-1}{S(k)} \ . \tag{45}$$

These last two equations are valid independently of whether the elementary diagrams are included or not.

The *simplest elementary diagram*, shown in Fig. 9, has four points and a symmetry factor 1/2. Actually, there is no way to sum up the contribution of all the elementary diagrams in a closed form, and so one has to rely on suitable approximations. It is customary to classify the HNC scheme according to the type of elementary diagrams included. For instance HNC/4 means that only the four points elementary diagram E_4 is implemented. Stated as it is, the HNC/4 scheme would only include one elementary diagram out of the infinite number one can draw by adding more and more internal points. This is not the case if one replaces the $h(r)$ bonds in E_4 by dressed lines $g(r)-1$. Since $g(r)$ already contains an infinite sum of diagrams, the dressed E_4 built in this way becomes a massive sum of elementary contributions, thus yielding a *better* approximation to the exact result. In this way, the dressed E_4 has to be recalculated at each iteration in the HNC scheme until convergence is reached. Alternatively, there has been a lot of work done in the HNC/5 scheme where a selected subset of all the possible five points elementary diagrams is included.

4 Optimized ground state

In the microscopic, variational theory the calculation of the ground state properties of the system of N particles with the mass m starts from the empirical Hamiltonian

$$H_0 = -\frac{\hbar^2}{2m}\sum_{i=1}^{N}\nabla_i^2 + \frac{1}{2}\sum_{i\neq j}^{N} V(|\mathbf{r}_i - \mathbf{r}_j|)\,. \tag{46}$$

One assumes that the two–particle interaction $V(|\mathbf{r}_i - \mathbf{r}_j|)$ is either known like the Coulomb interaction between charged particles or it is empirically determined as is the case with the interaction between helium atoms.

The variational problem is to minimize the total energy

$$E_0 = \frac{\langle\Psi_0|H_0|\Psi_0\rangle}{\langle\Psi_0|\Psi_0\rangle} \tag{47}$$

with respect to the n–particle densities of the system

$$\begin{aligned}&\rho_n(\mathbf{r}_1,\ldots\mathbf{r}_n) = \\ &= \frac{N!}{(N-n)!}\frac{1}{\langle\Psi_0|\Psi_0\rangle}\int d^3r_{n+1}\ldots d^3r_N|\Psi_0(\mathbf{r}_1,\ldots\mathbf{r}_N)|^2\,.\end{aligned} \tag{48}$$

In the homogeneous system with a constant density ρ_0 it is more convenient to use the n–particle distribution functions, which are normalized to unity when all particles are far apart,

$$g_n(\mathbf{r}_1,\ldots\mathbf{r}_n) = \frac{\rho_n(\mathbf{r}_1,\ldots\mathbf{r}_n)}{\rho_0^n}\,. \tag{49}$$

Following Feenberg's book [59] we start from the quadratic form

$$\begin{aligned}&X^{(n)}(\mathbf{r}_1,\ldots\mathbf{r}_n) \\ &= \frac{N!}{(N-n)!\langle\Psi_0|\Psi_0\rangle}\int d^3r_{n+1}\ldots d^3r_N\Psi_0(H-E_0)\Psi_0\,,\end{aligned} \tag{50}$$

and show that the right hand side of the equation can be expressed in terms of distribution functions. If these are correctly generated from the solution of the Schrödinger equation $H\Psi_0 = E_0\Psi_0$ then the right hand side vanishes defining the n–particle *Euler equation* of the system.

For the real wave function the kinetic energy part of the Hamiltonian can be written as

$$\frac{\hbar^2}{2m}\Psi_0\nabla^2\Psi_0 = \frac{\hbar^2}{8m}\nabla^2\Psi_0^2 + \frac{\hbar^2}{8m}\Psi_0^2\nabla^2\log(\Psi_0^2) \tag{51}$$

and the integrand in Eq. (51) becomes

$$\Psi_0(H-E_0)\Psi_0 = \left[-\frac{\hbar^2}{8m}\sum_{i=1}^{N}\nabla_i^2 - E_0\right. \tag{52}$$

$$+\frac{1}{2}\sum_{i\neq j}^{N} V(|\mathbf{r}_i-\mathbf{r}_j|)-\frac{\hbar^2}{8m}\sum_{i=1}^{N}\nabla_i^2\log\Psi_0^2\Bigg]\Psi_0^2\,.$$

It can be simplified by introducing a *generalized* β–dependent *square of the wave function*

$$\Psi_0^2(\mathbf{r}_1,\dots\mathbf{r}_N;\beta)=\ e^{\beta V_{JF}(\mathbf{r}_1,\dots\mathbf{r}_N)}\Psi_0^2(\mathbf{r}_1,\dots\mathbf{r}_N)\,. \tag{53}$$

and the *generalized normalization integral*

$$I_0(\beta)=\int d^3r_1\dots d^3r_N\ \Psi_0^2(\mathbf{r}_1,\dots\mathbf{r}_N)\ e^{\beta V_{JF}(\mathbf{r}_1,\dots\mathbf{r}_N)} \tag{54}$$

with the *Jackson–Feenberg effective potential*

$$V_{JF}(\mathbf{r}_1,\dots\mathbf{r}_N)=\frac{1}{2}\sum_{i\neq j}^{N} V(|\mathbf{r}_i-\mathbf{r}_j|)-\frac{\hbar^2}{8m}\sum_{i=1}^{N}\nabla_i^2\log\Psi_0^2\,. \tag{55}$$

Quantities which depend on the wave function like distribution functions become then β–dependent,

$$\begin{aligned}&\rho_n(\mathbf{r}_1,\dots\mathbf{r}_n;\beta)= \\ &=\frac{N!}{(N-n)!}\frac{1}{I_0(\beta)}\int d^3r_{n+1}\dots d^3r_N\Psi_0^2(\mathbf{r}_1,\dots\mathbf{r}_N;\beta)\,.\end{aligned} \tag{56}$$

The return to the original notation takes place by setting $\beta=0$ at the end of the calculation. In this notation the norm of the wave function is

$$I_0(0)=\langle\Psi_0|\Psi_0\rangle \tag{57}$$

and the total energy of the system is then simply

$$\begin{aligned}E_0&=\frac{d}{d\beta}\log I_0(\beta)\Big|_{\beta=0} \\ &=\frac{1}{\langle\Psi_0|\Psi_0\rangle}\int d^3r_1\dots d^3r_N\ \Psi_0^2(\mathbf{r}_1,\dots\mathbf{r}_N)\ V_{JF}(\mathbf{r}_1,\dots\mathbf{r}_N)\end{aligned} \tag{58}$$

The full integrand (52) assumes the form

$$\begin{aligned}&\frac{1}{I_0(0)}\Psi_0(H-E_0)\Psi_0= \\ &=\frac{d}{d\beta}\left[\frac{1}{I_0(\beta)}e^{\beta V_{JF}(\mathbf{r}_1,\dots\mathbf{r}_N)}\right]\Bigg|_{\beta=0}\Psi_0^2(\mathbf{r}_1,\dots\mathbf{r}_N) \\ &-\frac{\hbar^2}{8m}\frac{1}{I_0(0)}\sum_{i=1}^{N}\nabla_i^2\Psi_0^2(\mathbf{r}_1,\dots\mathbf{r}_N)\,.\end{aligned} \tag{59}$$

The quadratic equation can now be formally integrated giving

$$\begin{aligned} & X^{(n)}(\mathbf{r}_1, \dots \mathbf{r}_n) \\ &= \frac{N!}{(N-n)!}\frac{1}{I_0(0)} \int d^3 r_{n+1} \dots d^3 r_N \Psi_0 (H - E_0)\Psi_0 \,, \\ &= \frac{d}{d\beta}\rho_n(\mathbf{r}_1, \dots \mathbf{r}_n; \beta)\Big|_{\beta=0} - \frac{\hbar^2}{8m}\sum_{i=1}^{n} \nabla_i^2 \rho_n(\mathbf{r}_1, \dots \mathbf{r}_n; 0)\,. \end{aligned} \tag{60}$$

In the case of $n = 2$ if the Schrödinger equation is satisfied, then

$$X^{(2)}(\mathbf{r}_1, \mathbf{r}_2) = 0 \tag{61}$$

and we get the Euler equation for the radial distribution function $g(r) = \frac{1}{\rho_0^2}\rho_2(|\mathbf{r}_1 - \mathbf{r}_2|)$ as a function of radius $r = |\mathbf{r}_1 - \mathbf{r}_2|$

$$g'(r) \equiv \frac{d}{d\beta} g(r;\beta)\Big|_{\beta=0} = \frac{\hbar^2}{4m}\nabla^2 g(r;0)\,. \tag{62}$$

We have introduced here Feenberg's prime notation and ignored β from the list of arguments. This notation should not be mixed with the ordinary derivative with respect to the coordinate r. The Euler equation is valid for all real wave functions, but the main problem is to calculate the β–derivative term.

4.1 Euler equation with the Jastrow wave function

For the practical implementation of the Euler equation Eq. (62) we return to the Jastrow ansatz (27) for the wave function. Then the generalized normalization integral (54) becomes

$$I_0(\beta) = \int d^3 r_1 \dots d^3 r_N \;\; \exp\left[\sum_{i<j}^{N} u_2(|\mathbf{r}_i - \mathbf{r}_j|;\beta)\right] \,, \tag{63}$$

where we have defined the generalized correlation functions by adding the Jastrow correlation function into the Jackson–Feenberg potential (55),

$$u_2(r;\beta) \equiv u_2(r) + \beta \left[V(r) - \frac{\hbar^2}{4m}\nabla^2 u_2(r)\right] . \tag{64}$$

Its β–derivative is simple to calculate,

$$u_2'(r) \equiv \frac{\partial u_2(r;\beta)}{\partial \beta}\Big|_{\beta=0} = V(r) - \frac{\hbar^2}{4m}\nabla^2 u_2(r)\,. \tag{65}$$

The hypernetted chain (HNC) equation gives in terms of diagrams the connection between the correlation and distribution functions,

$$g(r) = e^{u_2(r)+N(r)+E(r)} \tag{66}$$

and the Ornstein–Zernike integral equation

$$N(|\mathbf{r}_1 - \mathbf{r}_2|) = \rho_0 \int d^3 r_3 (g(|\mathbf{r}_1 - \mathbf{r}_3|) - 1) X(|\mathbf{r}_3 - \mathbf{r}_2|) \tag{67}$$

sums the nodal diagrams, $N(r)$, which are formed by iterating the integral equation up to infinite order with the sum of composite diagrams $X(r)$,

$$X(r) = g(r) - 1 - N(r)\,. \tag{68}$$

The sum of elementary diagrams $E(r)$ must be calculated term by term. Typically one stops after the five–body diagrams.

From the HNC–equation (66) we can calculate the β–derivative of the radial distribution function

$$g'(r) = g(r)\left[u_2'(r) + N'(r) + E'(r)\right]\,. \tag{69}$$

Inserting here $u_2'(r)$ from Eq. (65) together with $u_2(r)$ solved from Eq. (66),

$$u_2(r) = \log g(r) - N(r) - E(r)\,, \tag{70}$$

we get

$$\begin{aligned} g'(r) &= g(r)\left(V(r) + N'(r) + E'(r)\right) \\ &- \frac{\hbar^2}{4m}\left[g(r)\ \nabla^2 \log g(r) - g(r)\left(\nabla^2 N(r) + \nabla^2 E(r)\right)\right]\,. \end{aligned} \tag{71}$$

It is useful to define two new quantities the *induced potential* $w_{\rm ind}(r)$ in terms of the sum of nodal diagrams $N(r)$,

$$w_{\rm ind}(r) \equiv N'(r) + \frac{\hbar^2}{4m}\nabla^2 N(r)\,, \tag{72}$$

and the *effective potential arising from the elementary diagrams*,

$$V_{\rm ele}(r) \equiv E'(r) + \frac{\hbar^2}{4m}\nabla^2 E(r)\,. \tag{73}$$

These simplify the expression of $g'(r)$ and if we furthermore use the identity

$$g(r)\ \nabla^2 \log g(r) = -\nabla^2 g(r) + 4\sqrt{g(r)}\ \nabla^2 \sqrt{g(r)} \tag{74}$$

then the Euler equation (62) can be written in the form of a zero–energy Schrödinger equation

$$-\frac{\hbar^2}{m}\nabla^2\sqrt{g(r)} + \left(V(r) + w_{\rm ind}(r) + V_{\rm ele}(r)\right)\sqrt{g(r)} = 0 \tag{75}$$

where $\sqrt{g(r)}$ plays the role of the wave function and the normalization is such that $\sqrt{g(\infty)} = 1$. Yet, one should realize that this equation is highly non–linear because both $w_{\rm ind}(r)$ and $V_{\rm ele}(r)$ depend on the solution $g(r)$.

The above formulation puts weight on the short range behavior of the radial distribution function. Especially for singular potentials $V(r)$ we can derive the behavior of $g(r)$ when $r \to 0$. In the case of the Coulomb potential — e^2/r with $e^2 = q^2/(4\pi\varepsilon_0)$ where q is the charge of the particles and ε_0 is the dielectric constant — $g(r)$ must satisfy the cusp condition

$$\frac{d}{dr}\log g(r) = \frac{e^2 m}{\hbar^2}\,. \tag{76}$$

In the case of the Lennard–Jones potential

$$V(r) = \epsilon\left[\left(\frac{\sigma}{r}\right)^{12} - \left(\frac{\sigma}{r}\right)^{6}\right] \tag{77}$$

$g(r)$ has an essential singularity at the origin

$$g(r) \overset{r\to 0}{\to} \exp\left[-\frac{A}{r^5}\right]; \qquad A = \frac{8}{5}\frac{m\sqrt{\epsilon}}{\hbar^2}\sigma^6\,. \tag{78}$$

Another way to solve the Euler equation (62), which put emphasis on the long wavelength behavior, is to define the *particle–hole effective interaction*,

$$V_{p-h}(r) \equiv X'(r) + \frac{\hbar^2}{4m}\nabla^2 X(r)\,, \tag{79}$$

in terms of the sum of composite diagrams $X(r)$ and its β–derivative from Eq. (68)

$$X'(r) = g'(r) - N'(r)\,. \tag{80}$$

We can write Eq. (71) into a new form by subtracting $N'(r)$ from both sides, inserting the definitions (72) and (73) and using another identity for the logarithmic term

$$g(r)\nabla^2 \log g(r) = \nabla^2 g(r) - 4\left(\sqrt{g(r)}\right)^2\,. \tag{81}$$

This leads to the expression

$$\begin{aligned} X'(r) &= g(r)\left[V(r) + V_{\text{ele}}(r)\right] + \left[g(r) - 1\right] w_{\text{ind}}(r) \\ &\quad + \frac{\hbar^2}{4m}\left[4\left(\nabla\sqrt{g(r)}\right)^2 - \nabla^2 X(r)\right]\,. \end{aligned} \tag{82}$$

Combining this with the definition (79) we arrive at the expression for the particle–hole potential

$$\begin{aligned} V_{p-h}(r) &= g(r)\left[V(r) + V_{\text{ele}}(r)\right] \\ &\quad + \left[g(r) - 1\right] w_{\text{ind}}(r) + \frac{\hbar^2}{m}\left(\nabla\sqrt{g(r)}\right)^2\,. \end{aligned} \tag{83}$$

For the homogeneous system it is often more convenient to *work in momentum space* and define the structure function $S(k)$ as the Fourier transform of $g(r)-1$,

$$S(k) = 1 + \rho_0 \int d^3r \; (g(r)-1) \; e^{-i\mathbf{k}\cdot\mathbf{r}} \, . \tag{84}$$

Similarly we get the Fourier transform of the β–derivative

$$S'(k) = \rho_0 \int d^3r \; g'(r) \; e^{-i\mathbf{k}\cdot\mathbf{r}} \, . \tag{85}$$

With these Fourier transforms the Euler equation (62) can be written in the momentum space

$$S'(k) = -\frac{\hbar^2 k^2}{4m} \left(S(k)-1\right) \, . \tag{86}$$

The Ornstein–Zernike equation (67) contains the convolution integral, which is of a product form in the Fourier space and can be solved easily together with Eq. (68) giving

$$\tilde{X}(k) = 1 - \frac{1}{S(k)} \, . \tag{87}$$

Performing the β–derivative operation and using the Eq. (86) we get

$$\tilde{X}'(k) = \frac{S'(k)}{S^2(k)} = -\frac{\hbar^2 k^2}{4m} \frac{(S(k)-1)}{S^2(k)} \, . \tag{88}$$

Inserting these into the Fourier transform of the definition (79) we find a simple expression for $\tilde{V}_{\mathrm{p-h}}(k)$

$$\begin{aligned} \tilde{V}_{\mathrm{p-h}}(k) &= \tilde{X}'(k) - \frac{\hbar^2 k^2}{4m} \tilde{X}(k) \\ &= -\frac{\hbar^2 k^2}{4m} \left(\frac{S(k)-1}{S^2(k)} + \frac{S(k)-1}{S(k)} \right) \\ &= -\frac{\hbar^2 k^2}{4m} \left(1 - \frac{1}{S^2(k)} \right) \, , \end{aligned} \tag{89}$$

which can be solved for the structure function and we get the *Bogoljubov–like form of the Euler equation*

$$S(k) = \frac{k}{\sqrt{k^2 + \frac{4m}{\hbar^2} \tilde{V}_{\mathrm{p-h}}(k)}} \, . \tag{90}$$

We still need to calculate the induced potential $w_{ind}(r)$ defined in Eq. (72). From Eqs. (68) and (87) we get

$$\tilde{N}(k) = \frac{(S(k)-1)^2}{S(k)} \, . \tag{91}$$

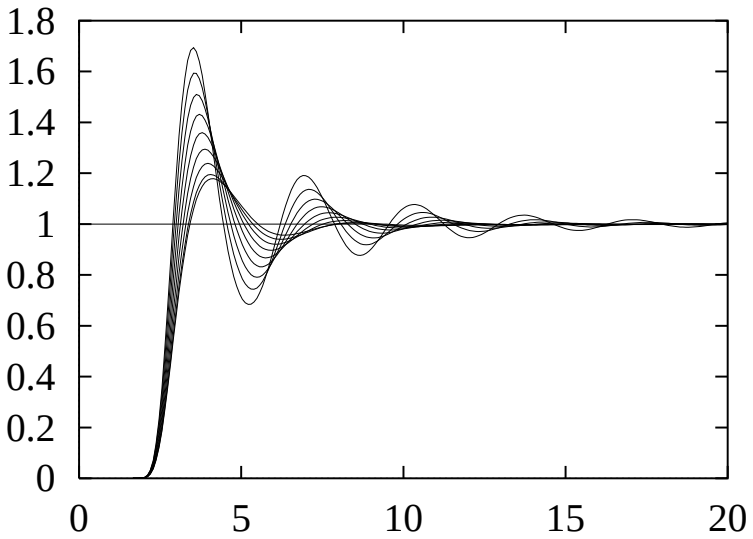

Figure 10: Radial distribution functions around saturation density in 3D ^{4}He.

The β–derivative and the use of Eqs. (86) and (88) gives

$$\begin{aligned}\tilde{N}'(k) &= S'(k) - \tilde{X}'(k) \\ &= -\frac{\hbar^2 k^2}{4m}\frac{(S(k)-1)^2\,(S(k)+1)}{S^2(k)}\,.\end{aligned} \tag{92}$$

Inserting these into the definition (72) we get the Fourier transform of $w_{ind}(r)$

$$\begin{aligned}\tilde{w}_{ind}(k) &= \tilde{N}'(k) - \frac{\hbar^2 k^2}{4m}\tilde{N}(k) \\ &= -\frac{\hbar^2 k^2}{4m}(S(k)-1)^2\left(\frac{S(k)+1}{S^2(k)} + \frac{1}{S(k)}\right) \\ &= -\frac{\hbar^2 k^2}{4m}(2S(k)+1)\left(1-\frac{1}{S(k)}\right)^2\,.\end{aligned} \tag{93}$$

Equations (90), (84) and (93) form a self–consistent set of equations which can be solved iteratively.

In the the long wavelength limit the structure function of the ^{4}He liquid is linear and inversely proportional to the speed of sound c

$$S(k) \overset{k\to 0}{\to} \frac{\hbar k}{2mc}\,, \tag{94}$$

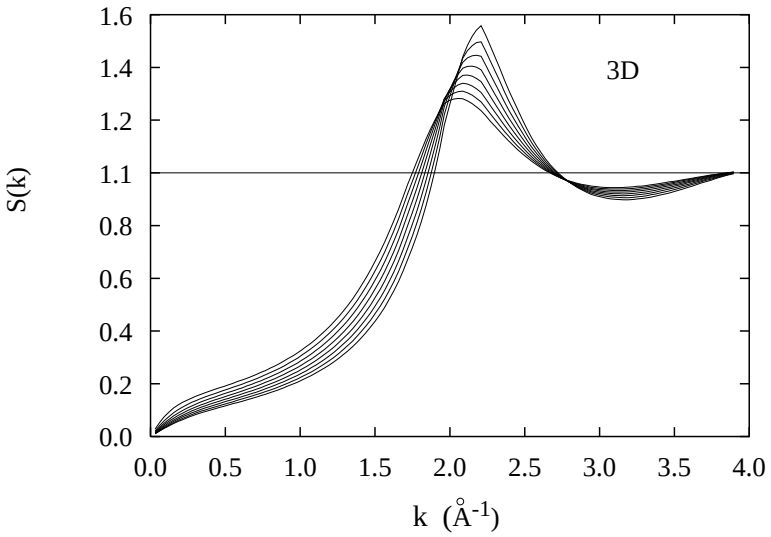

Figure 11: Static structure functions around saturation density in 3D ^{4}He.

which tells that $\tilde{V}_{\mathrm{p-h}}(0) = mc^2$. In the case of charged Bose gas the Coulomb interaction $4\pi e^2\rho_0/k^2$ dominates the small k behavior of $\tilde{V}_{\mathrm{p-h}}(k)$ and the structure function becomes quadratic

$$S(k) \overset{k\to 0}{\to} \frac{\hbar k^2}{2m\omega_p} \tag{95}$$

where $\omega_p = \sqrt{4\pi\rho_0 e^2/m}$ is the plasma frequency.

5 Dynamic structure of Bose fluids

In this section we study excited states. They can be accessed experimentally in essentially two ways: by increasing the temperature, and by exciting the system with an external probe as is done in neutron scattering. At finite temperature, the system populates some of the excited states and the elementary excitation spectrum is required if one seeks to understand the thermodynamic properties of the system. As en example, a quantity that directly depends on the density of excited states and therefore on the excitation energies is the specific heat. On the other hand, in a scattering event the probe transfers momentum and energy to the system, and the cross section for fixed momentum transfer as a function of E shows marked peaks at the excitation energies.

5.1 Low excited states

We begin the discussion of excitations with the Feynman model of the elementary excitation modes of a strongly correlated Bose system. Using a variational *ansatz*, Feynman [45] showed that, in the long wavelength limit, the wave function of the lowest excited states corresponding to a momentum $\mathbf{k}$ takes the form

$$\mid \Psi_{\mathbf{k}}\rangle = \rho_{\mathbf{k}} \mid \Psi_0\rangle \ , \tag{96}$$

where Ψ_0 is assumed to be the *exact* ground state and

$$\rho_{\mathbf{k}} = \sum_j e^{i\mathbf{k}\cdot\mathbf{r}_j} \tag{97}$$

is the operator exciting density oscillation of wavelength $\mathbf{k}$. The excitation energy associated with this trial wave function becomes then an upper bound to the exact excitation energy.

Taking into account that

$$\rho^\dagger_{\mathbf{k}}\rho_{\mathbf{k}} = \sum_i e^{-i\mathbf{k}\cdot\mathbf{r}_i} \sum_j e^{i\mathbf{k}\cdot\mathbf{r}_j} = N + \sum_{i\neq j} e^{i\mathbf{k}\cdot(\mathbf{r}_j-\mathbf{r}_i)} \ , \tag{98}$$

where N is the number of particles, the normalization constant becomes

$$\frac{\langle \Psi_{\mathbf{k}} \mid \Psi_{\mathbf{k}}\rangle}{\langle \Psi_0 \mid \Psi_0\rangle} = NS(k) \tag{99}$$

Here $S(k)$ is the Fourier transform of the radial distribution function $g(r)$ of the ground state from Eq. (84).

The excitation energy can then be written as follows,

$$\begin{aligned} \epsilon(k) &= \frac{\langle \Psi_{\mathbf{k}} \mid H - E_0 \mid \Psi_{\mathbf{k}}\rangle}{\langle \Psi_{\mathbf{k}} \mid \Psi_{\mathbf{k}}\rangle} \\ &= \frac{\langle \Psi_0 \mid \rho^\dagger_{\mathbf{k}} \left(H - E_0\right) \rho_{\mathbf{k}} \mid \Psi_0\rangle}{\langle \Psi_0 \mid \rho^\dagger_{\mathbf{k}}\rho_{\mathbf{k}} \mid \Psi_0\rangle} \end{aligned} \tag{100}$$

which, after shifting the position of the rightmost density fluctuation operator, leads to

$$\begin{aligned} \epsilon(k) = &\frac{\langle \Psi_0 \mid \rho^\dagger_{\mathbf{k}}\rho_{\mathbf{k}} \left(H - E_0\right) \mid \Psi_0\rangle}{\langle \Psi_0 \mid \rho^\dagger_{\mathbf{k}}\rho_{\mathbf{k}} \mid \Psi_0\rangle} \\ &+ \frac{\langle \Psi_0 \mid \rho^\dagger_{\mathbf{k}} \left[(H - E_0), \rho_{\mathbf{k}}\right] \mid \Psi_0\rangle}{\langle \Psi_0 \mid \rho^\dagger_{\mathbf{k}}\rho_{\mathbf{k}} \mid \Psi_0\rangle} \ . \end{aligned} \tag{101}$$

The first term of the previous equation is zero when $\mid \psi_0\rangle$ is the exact ground state but also when it is a variational model fulfilling the two–body optimization condition of Eq. (61).

As for the second term, the commutator of $\rho_{\mathbf{k}}$ with E_0 is trivially zero and, if the potential is momentum independent, the commutator with the potential

operator also cancels. In this way one is left with the kinetic energy contribution

$$\epsilon(k) = \frac{\langle \Psi_0 \mid \rho_{\mathbf{k}}^\dagger [-\frac{\hbar^2}{2m} \sum_i \nabla_i^2, \rho_{\mathbf{k}}] \mid \Psi_0 \rangle}{\langle \Psi_{\mathbf{k}} \mid \Psi_{\mathbf{k}} \rangle} \tag{102}$$

which can be easily simplified in the following way: Take into account the anti–hermitian character of the ∇ operator, and the fact that the ground state of a Bose system is always real, then

$$\int d\mathbf{R}\, \Psi_0 f(r)(\nabla_1 \Psi_0) = -\frac{1}{2} \int d\mathbf{R}\, \Psi_0 (\nabla_1 f) \Psi_0 \tag{103}$$

This together with the properties of commutators, allows us to write excitation energy

$$\epsilon(k) = \frac{\hbar^2}{2m} \sum_{i=1}^{N} \frac{\langle \Psi_0 \mid (\nabla_i \rho_{\mathbf{k}}^\dagger)(\nabla_i \rho_{\mathbf{k}}) \mid \Psi_0 \rangle}{\langle \Psi_0 \mid \Psi_0 \rangle} \left(\frac{\langle \Psi_{\mathbf{k}} \mid \Psi_{\mathbf{k}} \rangle}{\langle \Psi_0 \mid \Psi_0 \rangle} \right)^{-1} \tag{104}$$

thus leading to

$$\epsilon(k) = \frac{\hbar^2 k^2}{2m} \sum_{i}^{N} \left(\frac{\langle \Psi_{\mathbf{k}} \mid \Psi_{\mathbf{k}} \rangle}{\langle \Psi_0 \mid \Psi_0 \rangle} \right)^{-1} = \frac{\hbar^2 k^2}{2mS(k)} \ . \tag{105}$$

Recalling the small k behavior of $S(k)$ of Eq. (94) in helium, one finally recovers

$$\epsilon(k)_{k \to 0} = \hbar k c \tag{106}$$

which is the typical linear dispersion relation of phonon excitations.

The excitation spectrum of the system can be explored by means of *inelastic neutron scattering*. The setup of a typical scattering experiment is shown in Fig. 12. A beam of neutrons is emitted from the source, and falls on the sample after it is collimated to match the desired energy and momentum. Neutron detectors are placed at a large distance surrounding the sample. The scattering angle is directly related to the energy E and the momentum $\mathbf{q}$ transferred from the probe to the sample. An important aspect to bear in mind is the fact that the range of energies and momenta of the neutrons used in the experiment are precisely those matching the energies and momenta characteristic of the elementary excitations and collective modes of a typical condensed matter system.

In addition, the neutrons only interact with the nucleus of the atoms in the sample, and the nuclear interaction is really short–ranged compared with the wave length of the incident beam (of the order of few Å). This fact implies that the scattering basically happens in s–wave and that the effective potential the neutron sees can be well characterized by a *Fermi pseudo potential*

$$V(r) = \frac{2\pi\hbar^2}{m} b \sum_{j=1}^{N} \delta(\mathbf{r} - \mathbf{r}_j) \ , \tag{107}$$

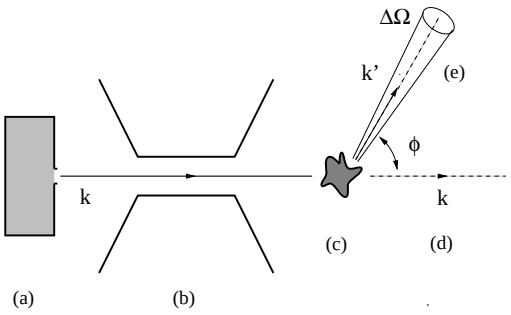

Figure 12: Experimental setup of a typical neutron scattering experiment. (a) neutron source, (b) momentum selector, (c) sample, (d) transmitted neutrons, (e) neutrons with momentum **k**' scattered in a solid angle $\Delta\Omega$.

where b is the scattering length. On the other hand, the use of Fermi' "Golden Rule" allows to write the cross–section in the form

$$\frac{d^2\sigma}{dEd\Omega} = \frac{k_1}{k_0} b^2 S(q,E) \ , \tag{108}$$

where $S(q,E)$ is the dynamic structure function

$$S(q,E) = \frac{1}{N} \sum_n \mid \langle n \mid \rho_{\mathbf{q}} \mid 0 \rangle \mid^2 \delta(E - (E_n - E_0)) \ , \tag{109}$$

$\rho_{\mathbf{q}}$ being the density fluctuation operator.

The measurement performed at each detector can be associated with well defined values of the energy and momentum transferred, and the number of counts registered in each detector gives precise information about the intensity of the scattering. This intensity is characterized by the double differential cross section defined above, which becomes the product of a kinematic term containing the initial and the final momentum of the neutron, the scattering length that defines the interaction, and the new function, $S(q,E)$, which incorporates all the information one can extract in the experiment corresponding to the system under study. The dynamic structure function for a given excitation operator collects the contribution of all excited states which are accessible with that excitation operator, and that are compatible with the external energy and momentum being transferred to the system. The cross section then presents marked peaks at these energies.

As an example, one can calculate $S(q,E)$ in the one–phonon approximation, where $\rho_{\mathbf{q}} \mid 0\rangle$ are the only allowed excited states. This is a very crude approximation, but since this *ansatz* gives a good description of the spectrum at very low energies, one can expect the resulting $S(q,E)$ to be accurate enough to describe the response in this regime.

The set of normalized excited states considered are then

$$\mid n\rangle \equiv \frac{\mid \Psi_{\mathbf{k}}\rangle}{\langle \Psi_{\mathbf{k}} \mid \Psi_{\mathbf{k}}\rangle^{1/2}} = \frac{\rho_{\mathbf{k}} \mid \Psi_0\rangle}{N^{1/2} S(k)^{1/2}} \ , \tag{110}$$

and the required matrix elements become

$$\langle n \mid \rho_{\mathbf{q}} \mid \ 0\rangle = \delta_{\mathbf{k},\mathbf{q}} N^{1/2} (S(q))^{1/2} \ , \tag{111}$$

which lead to the expression

$$S(q,E) = \frac{1}{N} \sum_{\mathbf{k}} \delta_{\mathbf{kq}} N S(q) \delta \left(E - \frac{\hbar^2 k^2}{2mS(k)} \right) \ . \tag{112}$$

Now, one can use the $\delta_{\mathbf{kq}}$ to perform the summation over $\mathbf{k}$ to finally find

$$S(q,E) = S(q) \delta \left(E - \frac{\hbar^2 q^2}{2mS(q)} \right) \ . \tag{113}$$

In this approximation, $S(q,E)$ becomes a δ-function centered at the excitation energy with a strength given by the static structure function $S(q)$. There is only one excited state taking all the strength of the excitation operator because in this approximation there is only one state able to take the whole momentum and energy transferred to the system.

Furthermore, one can also perform an analysis in terms of the *energy weighted sum rules* satisfied by $S(q,E)$, which is a common tool used to study the dynamic structure function of generic systems. This is done by evaluating the different energy moments of $S(q,E)$ and inferring its behavior from them. Sum rules of the response are defined as

$$m_k(q) = \int_0^\infty dE \, E^k S(q,E) \ , \tag{114}$$

which, due to the energy integration, do not depend on the detailed structure of the excited states and reduce to ground state expectation values of commutators of the Hamiltonian and the density fluctuation operator.

Here only the first two moments m_0 and m_1 will be considered. The idea is to first carry out the energy integration and to use the closure property when appropriate. The m_0 moment is extremely simple and becomes

$$\begin{aligned} m_0(q) &= \int dE \, S(q,E) \\ &= \frac{1}{N} \int dE \sum_n \mid \langle n \mid \rho_{\mathbf{q}} \mid 0\rangle \mid^2 \delta(E - (E_n - E_0)) \\ &= \frac{1}{N} \sum_n \mid \langle n \mid \rho_{\mathbf{q}} \mid 0\rangle \mid^2 \end{aligned}$$

$$= \frac{1}{N}\sum_n \langle 0 \mid \rho^\dagger_{\mathbf{q}} \mid n\rangle\langle n \mid \rho_{\mathbf{q}} \mid 0\rangle$$
$$= \frac{1}{N}\langle 0 \mid \rho^\dagger_{\mathbf{q}}\rho_{\mathbf{q}} \mid 0\rangle = S(q)\ . \tag{115}$$

The evaluation of $m_1(q)$ is also straightforward

$$\begin{aligned} m_1 &= \int_0^\infty dE\, S(q,E)\, E \\ &= \frac{1}{N}\sum_n (E_n - E_0)\langle 0 \mid \rho^\dagger_{\mathbf{q}} \mid n\rangle\langle n \mid \rho_{\mathbf{q}} \mid 0\rangle \\ &= \frac{1}{N}\sum_n \langle 0 \mid \rho^\dagger_{\mathbf{q}} \mid n\rangle\langle n \mid [H,\rho_{\mathbf{q}}] \mid 0\rangle \\ &= \frac{1}{2}\frac{1}{N}\langle 0 \mid [\rho^\dagger_{\mathbf{q}},[H,\rho_{\mathbf{q}}]] \mid 0\rangle \end{aligned} \tag{116}$$

where in the last step use has been made of the time reversal invariance of the system. [46]

Only the kinetic operator from H contributes to the innermost commutator, and after little algebra one finds the final result

$$m_1(q) = \frac{\hbar^2 q^2}{2m}\ , \tag{117}$$

thus showing that the first moment of the response, also known as the *f-sum rule*, depends on the details of the system only through the mass of its constituents.

Notice that this result has been obtained on the basis that the system is initially in its ground state, and that it is infinite, homogeneous and invariant under time reversal transformations. These conditions are quite common and therefore the range of validity of this sum rule is quite wide. Of course, the fact that $m_1(q) = \hbar^2 q^2/2m$ is very interesting from the theoretical point of view as it imposes a *severe model independent constraint* on any realistic calculation of the response.

At this point it is straightforward to check that $S(q,E)$ calculated in the one–phonon approach, $S(q,E) = S(q)\delta(E - \hbar^2 q^2/2mS(q))$, fulfills these two sum rules. Of course, this fact does not mean that this is the exact response. Actually, one can reverse the question and ask what should the form of $S(q,E)$ be if the sum rule is exhausted by only one state. In that case, one can write

$$S(q,E) = Z(q)\delta(E - E_q) \tag{118}$$

and require the two first sum rules to be fulfilled

$$m_0(q) = \int_0^\infty S(q,E)\, dE = S(q) \equiv Z(q) \tag{119}$$

and

$$m_1(q) = \int_0^\infty S(q,E) E\, dE = \frac{\hbar^2 q^2}{2m} \equiv Z(q)E_q\ , \tag{120}$$

so that one can recover $E_q = m_1/m_0$ to get $E_q = \hbar^2 q^2/2mS(q)$. This shows that the one–phonon approximation is the exact solution in this case when only one state is populated.

5.2 Linear response and equation of motion method

In the calculation of the ground state properties we optimized the total energy and derived the Euler equations for the pair distribution function.

In this section we follow a similar approach for the dynamic, time dependent system and optimize the action integral with respect to density oscillations. Time dependence is introduced into the system by adding an external, driving potential into the Hamiltonian. The bosonic quantum system responds to that by changing its density. Since the Hamiltonian is known and the wave function is solved from the least action principle we can derive the continuity equations for the one– and two–particle currents and densities, which are the equations of motion of the system. In this approach all particles are treated on the same footing including those which are in the Bose condensed state. The fraction of particles in the condensate can be calculated from the asymptotic behavior of the dynamic structure function at large momenta and frequencies.

Let us assume that a quantum fluid is driven out of the ground state by an infinitesimal external interaction $\tilde{U}_{\rm ext}(k,\omega)$, with a given frequency ω and wave number k representing a probe. Under these assumptions we need to consider the linear response of th system and each Fourier component $\tilde{U}_{\rm ext}(k,\omega)$ of the interaction acts independently: a given component induces a density fluctuation, $\delta\tilde{\rho}_1(k,\omega)$, in the originally homogeneous system having the same wave vector and frequency. In particular, we choose to study a harmonic perturbation. We can do this without loss of generality, because every periodic perturbation can be Fourier decomposed into its harmonic components.

A probe with a given frequency produces transitions in the system transferring thus energy into it. This will heat up the system, even to such an extend that the system deformation can no longer be considered small and nonlinear effects become important. To avoid this, we adopt the usual idea of *adiabatically turning on the interaction*. Mathematically it amounts to multiplying the interaction by a factor $e^{\eta t}$, where η is a positive infinitesimal constant, set to zero at the end of the calculation. This procedure ensures also that the response to the prope is *causal* – i.e. the response occurs after the applied perturbation in time. For $t \to -\infty$, the system is in its ground state.

The response of the system is assumed to be linear and the information on its dynamic properties, excitations and decay modes, is contained in the density–density linear–response function defined as

$$\chi(k,\omega) = \frac{\delta\tilde{\rho}_1(k,\omega)}{\rho_0\tilde{U}_{\rm ext}(k,\omega)}\,. \tag{121}$$

A standard application of the first-order time-dependent perturbation theory, in which one treats the external potential as perturbation and projects the

state $|\Psi, \mathbf{k}\rangle$ onto the eigenstates of the unperturbed Hamiltonian, allows the linear response function to be written in terms of the eigenstates of the system as

$$\chi(k,\omega) = \frac{1}{N}\sum_n |\ \langle n\ |\ \rho_{\mathbf{k}}\ |\ 0\rangle\ |^2 \times \left[\frac{1}{\hbar\omega - \hbar\omega_{n0} + i\eta} - \frac{1}{\hbar\omega + \hbar\omega_{n0} + i\eta}\right] \tag{122}$$

Comparing with Eq.(109) we get

$$\chi(k,\omega) = \int d(\hbar\omega')S(k,\omega') \times \left[\frac{1}{\hbar\omega - \hbar\omega' + i\eta} - \frac{1}{\hbar\omega + \hbar\omega' + i\eta}\right] \tag{123}$$

The dynamic structure function thus serves as a *spectral density* for the density-density response function. At zero temperature the dynamic structure function gives the density-fluctuation excitation spectrum as a positive definite function defined on the positive real axis, and, therefore, contains the physical information in a more compact form than the linear density-density response function.

Recalling Plemelj's formula for singular integrals

$$\lim_{\eta\to 0}\frac{1}{\hbar\omega - \hbar\omega' \pm i\eta} = \mathcal{P}\frac{1}{\hbar\omega - \hbar\omega'} \mp i\pi\delta(\hbar\omega - \hbar\omega') \tag{124}$$

where $\mathcal{P}$ denotes Caychy principal value, we can split the linear response function into real and imaginary parts.

$$\begin{aligned}\mathcal{R}e\chi(k,\omega) &= \int_{-\infty}^{-\infty} d(\hbar\omega')S(k,\omega')\mathcal{P}\left(\frac{2\hbar\omega}{\hbar^2\omega^2 - \hbar^2\omega'^2}\right)\\ \mathcal{I}m\chi(k,\omega) &= -\pi\left[S(k,\omega') - S(k,-\omega')\right]\end{aligned} \tag{125}$$

The dynamic structure function measures real transitions induced by the probe, thus the imaginary (dissipative) part of the response function specifies directly the steady energy transfer from an oscillating probe to the many-particle system. The real (reactive) part describes virtual transition or reversible deformation of the system. We also see that the real part is an even function of ω, whereas the imaginary part is odd. At finite temperatures one must allow the possibility that the system transfer energy to the probe as well.

Eq. (125) connects the dynamic structure function, which provides a direct measure of the fluctuations in the system to the imaginary part of the linear response function describing energy dissipation. The relation between these two

in principle quite different phenomena is known as the *fluctuation–dissipation theorem*. At zero temperature $\omega > 0$ and $S(k, -\omega)$ vanishes and we can write

$$S(k,\omega) = -\frac{1}{\pi}\Im m\left[\chi(k,\omega)\right]. \tag{126}$$

Hence, $S(k,\omega)$ is known, once the relation between the one–body density fluctuations and the perturbation has been established and one can compare the theoretical results with experiments.

The dynamic structure function is measured in (x–ray, neutron) *scattering experiments* and provides information of the strength, lifetime, and dispersion of excitations. At low temperatures it consists typically of a low–frequency sharp peak and of a high–frequency broad contribution.[79, 51] It is therefore customary to write

$$S(k,\omega) = Z(k)\delta(\hbar\omega - \hbar\omega_0(k)) + S_{\rm mp}(k,\omega). \tag{127}$$

This suggests that Eq. (109) may not be the best way to formulate the dynamic structure of a strongly correlated system.

Eq. (123) expresses the linear response function in the *Kubo form*, in terms of the exact eigenstates of the system. These are something we do not know and thus some form of perturbation theory is needed.

Another method is to take the *Kubo form as Green's function* of the propagating density fluctuation (phonon Green's function). Then we can return to the diagrammatic techniques developed by Feynman and Dyson. We key quantity in *Dyson equations* is the *self-energy* $\Sigma(k,\omega)$ which is connected to the Green's function and similarly to the linear response function as follows,

$$\chi(k,\omega) = S(k)\Big[\frac{1}{\hbar\omega - \varepsilon(k) - \Sigma(k,\omega)} - \frac{1}{\hbar\omega + \varepsilon(k) + \Sigma^*(k,-\omega)}\Big]. \tag{128}$$

Here $\varepsilon(k)$ is the energy of a single collective mode. The above form is familiar from the *random phase approximation (RPA)* where the self energy contains a set of ring diagrams is summed up to infinite order. The form preserves the symmetry properties of the Kubo form.

The self–energy $\Sigma(k,\omega)$ is a complex quantity,

$$\Sigma(k,\omega) = \Delta(k,\omega) - i\Gamma(k,\omega). \tag{129}$$

Recalling that for singular integrand one has

$$\frac{1}{\omega - \omega'} = \mathcal{P}\frac{1}{\omega - \omega'} - i\pi\delta(\omega - \omega') \tag{130}$$

where $\mathcal{P}$ denotes the Cauchy principal value, we see that the dynamic structure function (126) has contributions from the *poles of the response function* and from the *imaginary part of the self–energy*.

The *elementary excitation modes* are determined by the positive frequency poles $\omega = \omega_0(k)$ of Eq. (128). We show in a moment that the poles lie on the real axis, then

$$\hbar\omega_0(k) = \varepsilon(k) + \Delta(k, \omega_0(k)) \tag{131}$$

and $\Gamma(k, \omega_0(k)) = 0$. The strength $Z(k)$ of that pole can then be evaluated from the derivative of the self–energy,

$$Z(k) = S(k) \left[1 - \left. \frac{d\Delta(k,\omega)}{d(\hbar\omega)} \right|_{\omega=\omega_0} \right]^{-1} . \tag{132}$$

The second term in (127), $S_{\rm mp}(k,\omega)$, is the *multi–phonon background*, *i.e.* the contribution in which a projectile like a neutron probing the system exchanges energy with two or more excitation modes. This contribution is determined by the imaginary part of the self–energy

$$S_{\rm mp}(k,\omega) = \frac{1}{\pi} S(k) \frac{\Gamma(k,\omega)}{\left[\hbar\omega + \varepsilon(k) + \Delta(k,\omega)\right]^2 + \left[\Gamma(k,\omega)\right]^2} . \tag{133}$$

The dynamic structure function is a positive function for positive values of ω and that is why also $\Gamma(k,\omega)$ must be a non–negative function. For $\Gamma(k,\omega) > 0$ the energy $\hbar\omega$ transfered into the system has created such excitation modes, that can decay into other lower lying excitations within finite lifetime.

In addition, the *relative weight*, $Z(k)/S(k)$, gives the efficiency of scattering processes from a single collective excitation, as seen from the *zeroth–moment sum rule*

$$\int_0^\infty S(k,\omega) d(\hbar\omega) = S(k) . \tag{134}$$

In other words, it gives the fraction of available scattering processes going through a single collective mode at a given wave vector. If the only excitation in the system were the collective mode $\varepsilon(k)$, like in the Feynman approximation, then the ratio $Z(k)/S(k)$ would be one.

Let us return to the proof that all poles of the response function must lie on the real ω–axis and thus they determine the collective, elementary excitation modes of the system. The pole solution of Eq.(128) must satisfy the implicit equation

$$\hbar\omega_0(k) = \varepsilon_F(k) + \Sigma(k, \omega_0(k)) \tag{135}$$

We start the proof by assuming that ω_0 is complex,

$$\omega_0 = x_0 + iy_0 , \tag{136}$$

and show that this leads to a contradiction.[87]

The general requirement that the dynamic structure function must be positive implies that the imaginary part of the self–energy $\Gamma(k,\omega) \geq 0$ when $\omega \geq 0$

and zero otherwise. Using the Kramer–Kronig relations we can write the self–energy in the spectral form

$$\Sigma(k,\omega) = \frac{1}{\pi}\int_0^\infty d\omega' \frac{\Gamma(k,\omega')}{\omega-\omega'}\,. \tag{137}$$

If we make the assumption of Eq. (136) then the poles are given by the solutions of the equation

$$x_0 + iy_0 - \varepsilon_F(k) = \frac{1}{\pi}\int_0^\infty d\omega' \frac{\Gamma(k,\omega')}{x_0+iy_0-\omega'}\,. \tag{138}$$

Setting imaginary parts equal on both sides of the equation we get

$$1 = -\int_0^\infty \frac{d\omega'}{\pi}\;\; \frac{\Gamma(k,\omega')}{(x_0-\omega')^2+y_0^2}\,. \tag{139}$$

The right–hand side is always negative and the equation can never be satisfied. We can conclude that the poles must lie on the real ω–axis.

5.3 Time–dependent correlation functions

Let us proceed with the details of the time–dependent response of the system. If a weak, time dependent interaction perturbs the system then the ground–state wave function, $\Psi_0(\mathbf{r}_1,\ldots,\mathbf{r}_N)$, is modified accordingly and it becomes time dependent. For later use we separate in the notations the time dependent phase due to the unperturbed ground state energy

$$\Psi(\mathbf{r}_1,\ldots,\mathbf{r}_N;t) = e^{-iE_0t/\hbar}\Phi(\mathbf{r}_1,\ldots,\mathbf{r}_N;t)\,, \tag{140}$$

the change in the normalization due to the perturbation

$$\Phi(\mathbf{r}_1,\ldots,\mathbf{r}_N;t) = \frac{1}{\sqrt{\mathcal{N}(t)}}\;\phi(\mathbf{r}_1,\ldots,\mathbf{r}_N;t) \tag{141}$$

and the time dependence of the correlation functions

$$\phi(\mathbf{r}_1,\ldots,\mathbf{r}_N;t) = e^{\frac{1}{2}\delta U(\mathbf{r}_1,\ldots,\mathbf{r}_N;t)}\Psi_0(\mathbf{r}_1,\ldots,\mathbf{r}_N)\,. \tag{142}$$

One can think $\delta U(\mathbf{r}_1,...,\mathbf{r}_N;t)$ as a complex–valued excitation operator

$$\delta U(\mathbf{r}_1,...,\mathbf{r}_N;t) = \sum_i \delta u_1(\mathbf{r}_i;t) + \sum_{i<j}\delta u_2(\mathbf{r}_i,\mathbf{r}_j;t) \tag{143}$$

expanded in terms of one– and two–body correlation functions. The time–dependent one–body function $\delta u_1(\mathbf{r}_i;t)$ must be included into the description because dynamics will normally break the translational invariance of the system, but restricting the time dependence to the one–body component only would

lead directly to the Feynman theory of one–phonon excitations as we will show later. The time–dependent two–body component is significant in situations where the external field excites fluctuations of wavelengths comparable to the inter–particle distance, as explicitly demonstrated for liquid ^{4}He [77, 75, 76, 74, 63] and for the bosonic Coulomb systems[80].

In the previous section we showed that the optimized ground state $\Psi_0(\mathbf{r}_1, \ldots, \mathbf{r}_N)$ satisfies the Schrödinger equation

$$H_0\Psi_0 = E_0\Psi_0 \tag{144}$$

where H_0 is the ground state Hamiltonian given in Eq. (46) and E_0 is the ground state energy appearing in the phase factor of definition Eq. (140). In order to simplify notations we assume that the ground state wave function is normalized to unity

$$\langle\Psi_0|\Psi_0\rangle = 1\,. \tag{145}$$

The normalization factor in Eq. (141) has changed from that due to the time dependence of the correlation factors

$$\mathcal{N}(t) = \int d^3r_1 \ldots d^3r_N |\Psi_0(\mathbf{r}_1, \ldots \mathbf{r}_N)|^2 e^{\Re e[\delta U(\mathbf{r}_1, \ldots \mathbf{r}_N; t)]}\,. \tag{146}$$

5.4 Action integral

The time evolution of the wave function functions is governed by the least–action principle [81, 82]

$$\begin{aligned} \delta\mathcal{S} &= \delta \int_{t_0}^{t} dt\mathcal{L}(t) \\ &\equiv \delta \int_{t_0}^{t} dt \left\langle \Psi(t) \left| H(t) - i\hbar\frac{\partial}{\partial t} \right| \Psi(t) \right\rangle = 0 \end{aligned} \tag{147}$$

where the Hamiltonian

$$H(t) = H_0 + \hat{U}_{\rm ext}(t) \tag{148}$$

now contains, besides the ground–state Hamiltonian H_0, also the time dependent operator $\hat{U}_{\rm ext}(t) = \sum_{i=1}^{N} U_{\rm ext}(\mathbf{r}_i; t)$, which creates an external, infinitesimal disturbance into the system. This is exactly the term that provides us the relation between the one–body density fluctuations and the perturbation, needed to calculate the dynamic linear response.

Using the ground state Schrödinger equation (144) we can write the integrand in the form

$$\mathcal{L}(t) = \left\langle \Phi(t) \left| H - E_0 - \frac{\hbar}{2}\left(i\frac{\partial}{\partial t} + h.c.\right) \right| \Phi(t) \right\rangle$$

$$= \frac{1}{\mathcal{N}(t)} \left\langle \Psi_0 \left| e^{\frac{1}{2}\delta U^*(t)} [H_0, e^{\frac{1}{2}\delta U(t)}] \right| \Psi_0 \right\rangle$$

$$+ \left\langle \Phi(t) \left| -\frac{\hbar}{2} \left(i\frac{\partial}{\partial t} + h.c. \right) + \hat{U}_{ext}(t) \right| \Phi(t) \right\rangle . \tag{149}$$

With the notation h.c. we add the hermitian conjugation of the time–derivative operator.

The *potential energy term* commutes with $\delta U(t)$ and thus only the kinetic energy gives contribution to the commutator. This can be evaluated with a little bit of algebra,

$$\begin{aligned}
&\int d\tau \ \Psi_0 \ e^{\frac{1}{2}\delta U^*(t)} \nabla^2 \left(e^{\frac{1}{2}\delta U(t)} \ \Psi_0 \right) \\
&= \int d\tau \Psi_0 e^{\frac{1}{2}\delta U^*(t)} \nabla \cdot \left(\frac{1}{2} e^{\frac{1}{2}\delta U(t)} \Psi_0 \nabla \delta U(t) + e^{\frac{1}{2}\delta U(t)} \nabla \Psi_0 \right) \\
&= \int d\tau \left[-e^{\frac{1}{2}\delta U^*(t)} \left(\frac{1}{2} \Psi_0 \nabla \delta U^*(t) + \nabla \Psi_0 \right) \frac{1}{2} e^{\frac{1}{2}\delta U(t)} \Psi_0 \nabla \delta U(t) \right. \\
&+ \left. \Psi_0 e^{\Re e[\delta U(t)]} \left(\frac{1}{2} \nabla \Psi_0 \cdot \nabla \delta U(t) + \nabla^2 \Psi_0 \right) \right] \\
&= \int d\tau \left[-\frac{1}{4} |\Psi_0|^2 e^{\Re e[\delta U(t)]} \ |\nabla \delta U(t)|^2 + \Psi_0 e^{\Re e[\delta U(t)]} \nabla^2 \Psi_0 \right]
\end{aligned}$$

giving the result

$$\begin{aligned}
&\frac{1}{\mathcal{N}(t)} \left\langle \Psi_0 \left| e^{\frac{1}{2}\delta U^*(t)} [H_0, e^{\frac{1}{2}\delta U(t)}] \right| \Psi_0 \right\rangle \\
&= \frac{\hbar^2}{8m} \left\langle \Phi(t) \left| \sum_{j=1}^{N} |\nabla_j \delta U(t)|^2 \right| \Phi(t) \right\rangle .
\end{aligned} \tag{150}$$

The evaluation of the *time derivative* gives

$$\begin{aligned}
&-\frac{\hbar}{2} \left\langle \Psi_0 \left| \frac{e^{\frac{1}{2}\delta U^*(t)}}{\sqrt{\mathcal{N}(t)}} \left(i\frac{\partial}{\partial t} + h.c. \right) \frac{e^{\frac{1}{2}\delta U(t)}}{\sqrt{\mathcal{N}(t)}} \right| \Psi_0 \right\rangle \\
&= \frac{1}{2}\hbar \left\langle \Phi(t) \left| \Im m[\delta \dot{U}(t)] \right| \Phi(t) \right\rangle
\end{aligned} \tag{151}$$

where we have used the dot–notation $\dot{f}(t) = \frac{\partial f(t)}{\partial t}$. Collecting *all together* we have the integrand

$$\begin{aligned}
\mathcal{L}(t) = \Big\langle \Phi(t) \Big| &\frac{\hbar^2}{8m} \sum_{j=1}^{N} |\nabla_j \ \delta U(t)|^2 \\
&+ \frac{1}{2}\hbar \ \Im m[\delta \dot{U}(t)] + \hat{U}_{ext}(t) \Big| \Phi(t) \Big\rangle .
\end{aligned} \tag{152}$$

5.5 Least action principle

In the least–action principle we search for the correlation functions $\delta u_1(\mathbf{r}_1;t)$, $\delta u_2(\mathbf{r}_1,\mathbf{r}_2;t)$, etc, which minimize the action integral (148). The variation

$$\delta\mathcal{S} = \delta\int_{t_0}^{t} dt'\mathcal{L}(t') = 0 \tag{153}$$

with respect to a general correlation function $\delta u_n(\mathbf{r}_1,\ldots,\mathbf{r}_n;t)$, which depends on n coordinates and time gives

$$\begin{aligned}
&\int d^3r_{n+1}\ldots d^3r_N\Big[-\frac{\hbar^2}{8m}\sum_{j=1}^{n}\nabla_j\cdot\big(|\Phi(t)|^2\nabla_j\delta U(t)\big)\\
&-\frac{i\hbar}{4}\frac{\partial}{\partial t}|\Phi(t)|^2+\left(\frac{\hbar}{2}\Im m[\delta\dot{U}]+\hat{U}_{ext}\right)\frac{1}{\mathcal{N}(t)}\frac{\partial|\phi|^2}{\partial\delta U^*(t)}\Big]\\
&-\left\langle\Phi(t)\left|\frac{\hbar}{2}\,\Im m[\delta\dot{U}]+\hat{U}_{ext}\right|\Phi(t)\right\rangle\frac{1}{\mathcal{N}(t)}\frac{\partial\mathcal{N}(t)}{\partial\delta U^*(t)}\,.
\end{aligned} \tag{154}$$

The derivatives can be calculated from the definitions (141)

$$\begin{aligned}
\frac{\partial|\phi|^2}{\partial\delta U^*(t)} &= \frac{1}{2}|\phi|^2\\
\frac{1}{\mathcal{N}}\frac{\partial\mathcal{N}}{\partial\delta U^*(t)} &= \frac{1}{2}\int d^3r_{n+1}\ldots d^3r_N|\Phi(t)|^2\\
\frac{\partial}{\partial t}|\Phi(t)|^2 &= |\Phi(t)|^2\left[\Re e\delta\dot{U}-\int d^3r_1\ldots d^3r_N|\Phi(t)|^2\Re e\delta\dot{U}\right]
\end{aligned}$$

and the least action principle can be written in the form

$$\begin{aligned}
&\int d^3r_{n+1}\ldots d^3r_N\Big[-\frac{\hbar^2}{4m}\sum_{j=1}^{n}\nabla_j\cdot\big(|\Psi|^2\nabla_j\delta U(t)\big)\\
&+|\Psi|^2\left(-\frac{i\hbar}{2}\delta\dot{U}+\hat{U}_{ext}-\left\langle\Psi\left|-\frac{i\hbar}{2}\delta\dot{U}+\hat{U}_{ext}\right|\Psi\right\rangle\right)\Big]=0\,.
\end{aligned} \tag{155}$$

5.6 Many–particle densities and currents

In order to simplify the notations in Eq. (155) we generalize the definition of the n–particle density in Eq. (57) to the time dependent wave function,

$$\bar{\rho}_n(\mathbf{r}_1,\ldots\mathbf{r}_n;t) = \frac{N!}{(N-n)!}\int d\tau_{n+1}|\Psi(\mathbf{r}_1,\ldots\mathbf{r}_N;t)|^2\,. \tag{156}$$

with $d\tau_{n+1}\equiv d^3r_{n+1}\ldots d^3r_N$ In the linear response theory one assumes that the time dependent perturbation is infinitesimal and hence it is natural to separate the time dependent and independent parts of the density,

$$\bar{\rho}_n(\mathbf{r}_1,\ldots\mathbf{r}_n;t) = \rho_n(\mathbf{r}_1,\ldots\mathbf{r}_n)+\delta\rho_n(\mathbf{r}_1,\ldots\mathbf{r}_n;t)\,. \tag{157}$$

Expanding to the first order in $\delta U(t)$ we get

$$\delta\rho_n(\mathbf{r}_1,\dots\mathbf{r}_n;t) \approx \frac{N!}{(N-n)!}\int d\tau_{n+1}|\Psi_0|^2 \times \Re e\Big[\delta U(t) - \langle\Psi_0\,|\delta U(t)|\,\Psi_0\rangle\Big]\,. \tag{158}$$

The physical density is a real quantity, but in Eq. (155) the terms with the time derivative can be identified with the density if we generalize the above definition to the complex density fluctuations by removing the notation for the real part.

Similarly we define the n–particle current

$$\mathbf{j}_{n,j}(\mathbf{r}_1,\dots\mathbf{r}_n;t) = \frac{\hbar}{2mi}\frac{N!}{(N-n)!} \times \int d\tau_{n+1}\left[\Psi^*\nabla_j\Psi - \Psi\nabla_j\Psi^*\right]\,, \tag{159}$$

expand it to the first order in $\delta U(t)$

$$\mathbf{j}_{n,j}(\mathbf{r}_1,\dots\mathbf{r}_n;t) \approx \frac{\hbar}{2m}\frac{N!}{(N-n)!} \times \int d\tau_{n+1}|\Psi_0(\mathbf{r}_1,\dots\mathbf{r}_N)|^2\Im m\left[\nabla_j\;\delta U(t)\right] \tag{160}$$

and generalize the definition to complex currents as needed in Eq. 155). The second index in the definition of currents refers to the index of the differentiated coordinate.

5.7 One– and two–particle continuity equations

With the generalized definitions of Eqs. (159) and (161), the least action principle (155) can be separated into one– and two–particle continuity equations — the equations of motion of the system, [77, 75, 76]

$$\nabla_1\cdot\mathbf{j}_1(\mathbf{r}_1;t) + \delta\dot\rho_1(\mathbf{r}_1;t) = D_1(\mathbf{r}_1;t) \tag{161}$$

$$\nabla_1\cdot\mathbf{j}_{2,1}(\mathbf{r}_1,\mathbf{r}_2;t) + \nabla_2\cdot\mathbf{j}_{2,2}(\mathbf{r}_1,\mathbf{r}_2;t) + \delta\dot\rho_2(\mathbf{r}_1,\mathbf{r}_2;t) = D_2(\mathbf{r}_1,\mathbf{r}_2;t)\,. \tag{162}$$

On one-body level we leave out the second index as unnecessary.

Inserting the definition of the excitation operator (143) into the definition of the density (159) and using the complex notation we get the expression of the one–particle density fluctuations in terms of the two– and three–particle distribution functions (49)

$$\delta\rho_1(\mathbf{r}_1;t) = \rho_0\;\delta u_1(\mathbf{r}_1;t)$$

$$+\rho_0^2\int d^3r_2(g_2(\mathbf{r}_1,\mathbf{r}_2)-1)\delta u_2(\mathbf{r}_2;t) \tag{163}$$
$$+\rho_0^2\int d^3r_2\Big[g_2(\mathbf{r}_1,\mathbf{r}_2)\delta u_2(\mathbf{r}_1,\mathbf{r}_2;t)$$
$$+\frac{\rho_0}{2}\int d^3r_3\left(g_3(\mathbf{r}_1,\mathbf{r}_2,\mathbf{r}_3)-g_2(\mathbf{r}_2,\mathbf{r}_3)\right)\delta u_2(\mathbf{r}_2,\mathbf{r}_3;t)\Big]\,.$$

From the definition (159) it is easy to verify that the particle number is conserved in the fluctuations

$$\int d^3r\delta\rho_1(\mathbf{r})=0 \tag{164}$$

and that the sequential relation is satisfied,

$$\int d^3r_2\ \delta\rho_2(\mathbf{r}_1,\mathbf{r}_2;t)=(N-1)\ \delta\rho_1(\mathbf{r}_1;t)\,. \tag{165}$$

The one– and two–particle currents can be read out of Eq. (161). Using again the complex notation we get

$$\mathbf{j}_1(\mathbf{r}_1;t)=\frac{\hbar\rho_0}{2mi}\Big\{\nabla_1\delta u_1(\mathbf{r}_1;t) \tag{166}$$
$$+\rho_0\int d^3r_2g_2(\mathbf{r}_1,\mathbf{r}_2)\nabla_1\delta u_2(\mathbf{r}_1,\mathbf{r}_2;t)\Big\}\,.$$
$$\mathbf{j}_{2,1}(\mathbf{r}_1,\mathbf{r}_2;t)=\frac{\hbar\rho_0^2}{2mi}\Big\{g_2(\mathbf{r}_1,\mathbf{r}_2) \tag{167}$$
$$\times\left[\nabla_1\delta u_1(\mathbf{r}_1;t)+\nabla_1\delta u_2(\mathbf{r}_1,\mathbf{r}_2;t)\right]$$
$$+\rho_0\int d^3r_3g_3(\mathbf{r}_1,\mathbf{r}_2,\mathbf{r}_3)\nabla_1\delta u_2(\mathbf{r}_1,\mathbf{r}_3;t)\Big\}\,.$$

The currents also satisfy the sequential relation

$$\int d^3r_2\ \mathbf{j}_{2,1}(\mathbf{r}_1,\mathbf{r}_2;t)=(N-1)\ \mathbf{j}_1(\mathbf{r}_1;t)\,. \tag{168}$$

The terms which depend on the external potential are collected into the functions $D_1(\mathbf{r}_1;t)$ and $D_2(\mathbf{r}_1,\mathbf{r}_2;t)$ and they are the terms which drive excitations into the system,

$$D_1(\mathbf{r}_1;t)=\frac{2\rho_0}{i\hbar}\Big\{U_{\rm ext}(\mathbf{r}_1;t)$$
$$+\rho_0\int d^3r_2\Big[g_2(\mathbf{r}_1,\mathbf{r}_2)-1\Big]U_{\rm ext}(\mathbf{r}_2;t)\Big\} \tag{169}$$
$$D_2(\mathbf{r}_1,\mathbf{r}_2;t)=\frac{2\rho_0^2}{i\hbar}\Big\{g_2(\mathbf{r}_1,\mathbf{r}_2)\left[U_{\rm ext}(\mathbf{r}_1;t)+U_{\rm ext}(\mathbf{r}_2;t)\right]$$
$$+\rho_0\int d^3r_3\Big[g_3(\mathbf{r}_1,\mathbf{r}_2,\mathbf{r}_3)-g_2(\mathbf{r}_1,\mathbf{r}_2)\Big]U_{\rm ext}(\mathbf{r}_3;t)\Big\}\,. \tag{170}$$

6 Solving the continuity equations

Up to now, we have formulated the problem in terms of a Hamiltonian, a trial wave function, the least action principle, and we have derived two coupled continuity equations (161) and (163). What we still need to do is to find a way to actually solve those continuity equations for the unknown quantities $\delta u_1(\mathbf{r};t)$ and $\delta u_2(\mathbf{r}_1,\mathbf{r}_2;t)$; assuming that all ground state quantities are known. In the following we introduce various approximation schemes.

In the homogeneous system fluctuations are weak and it is more convenient to work in the Fourier space. We define the one–body Fourier transform and its inverse as

$$\begin{aligned}\mathcal{F}[f(\mathbf{r};t)] &= \rho_0 \int d^3r\ dt\ e^{-i(\mathbf{k}\cdot\mathbf{r}-\omega t)} f(\mathbf{r};t) \\ &= \tilde{f}(\mathbf{k};\omega) \\ \mathcal{F}^{-1}[\tilde{f}(\mathbf{k};\omega)] &= \int \frac{d^3k\ d\omega}{(2\pi)^4\rho_0} e^{i(\mathbf{k}\cdot\mathbf{r}-\omega t)} \tilde{f}(\mathbf{k};\omega) \\ &= f(\mathbf{r};t)\end{aligned} \tag{171}$$

and the two–body Fourier transforms in the form

$$\begin{aligned}&\mathcal{F}[f(\mathbf{r}_1,\mathbf{r}_2;t)] = \\ &= \rho_0^2 \int d^3r_1 d^3r_2\ dt\ e^{-i(\mathbf{k}\cdot\mathbf{R}+\mathbf{p}\cdot\mathbf{r}-\omega t)} f(\mathbf{r}_1,\mathbf{r}_2;t) \\ &\mathcal{F}^{-1}[\tilde{f}(\mathbf{k},\mathbf{p};t)] = \\ &= \int \frac{d^3k d^3p\ d\omega}{(2\pi)^7\rho_0^2} e^{i(\mathbf{k}\cdot\mathbf{R}+\mathbf{p}\cdot\mathbf{r}-\omega t)} \tilde{f}(\mathbf{k},\mathbf{p};\omega)\ .\end{aligned} \tag{172}$$

Here $\mathbf{R} = (\mathbf{r}_1+\mathbf{r}_2)/2$ is the center–of–mass vector and $\mathbf{r} = \mathbf{r}_1 - \mathbf{r}_2$ the relative position vector; $\mathbf{k}$ and $\mathbf{p}$ are the center–of–mass and relative momenta, respectively.

6.1 Feynman approximation

The simplest, physically consistent approximation is the Feynman approximation where we limit the time dependence to the one–body correlation function by setting $\delta u_2(\mathbf{r}_1,\mathbf{r}_2;t) = 0$. In this case, we need to solve only the first continuity equation (161). The one–body current reduces to

$$\mathbf{j}_1(\mathbf{r}_1;t) = \frac{\hbar\rho_0}{2mi}\nabla_1 \delta u_1(\mathbf{r}_1;t) \tag{173}$$

and the time–dependent part of the density is simply

$$\begin{aligned}\delta\rho_1(\mathbf{r}_1;t) &= \rho_0 \delta u_1(\mathbf{r}_1;t) \\ &+ \rho_0^2 \int d^3r_2 \Big[g_2(|\mathbf{r}_1-\mathbf{r}_2|) - 1\Big] \delta u_1(\mathbf{r}_2;t)\,.\end{aligned} \tag{174}$$

The Fourier transforms into the momentum space can be readily calculated, resulting in

$$\delta\tilde{\rho}(k,t) = S(k)\rho_0\delta\tilde{u}(k,t)\,. \tag{175}$$

Inserting these results into the continuity equation (161), along with the Fourier transform of $D_1(\mathbf{r};t)$, we end up with

$$\left(-\varepsilon_F(k) + i\hbar\frac{\partial}{\partial t}\right)\delta\tilde{\rho}(k,t) = 2\rho_0 S(k)\tilde{U}_{\rm ext}(\mathbf{k},t)\,. \tag{176}$$

where we have used the notation

$$\varepsilon_F(k) = \frac{\hbar^2k^2}{2mS(k)}\,. \tag{177}$$

The external potential is part of the Hamiltonian and that is why it must be a real function. As discussed earlier without loss of generality we may take a harmonic perturbation with a fixed frequency dependence, ω,

$$U_{\rm ext}(\mathbf{r}_i;t) = U_e(\mathbf{r}_i,\omega)\cos(\omega t)e^{\eta t}, \qquad \eta\to 0+ \tag{178}$$

The time dependence is switched on adiabatically using a small, positive parameter η, which can be set equal to zero at the end of the calculations. In momentum space that is simply

$$\tilde{U}_{\rm ext}(\mathbf{k};t) = \tilde{U}_e(\mathbf{k},\omega)\cos(\omega t)e^{\eta t}\,. \tag{179}$$

The density response of the fluid has two components

$$\delta\tilde{\rho}(\mathbf{k},t) = \left[a(\mathbf{k},\omega)e^{-i\omega t} + b(\mathbf{k},-\omega)e^{i\omega t}\right]e^{\eta t}\,, \tag{180}$$

which can be different for ω and $-\omega$.

Inserting this into Eq. (176) and requiring that the solution must be valid for all t we can solve a and b,

$$\begin{aligned} a(\mathbf{k},\omega) &= \frac{\rho_0 S(k)\tilde{U}_e(\mathbf{k},\omega)}{\hbar\omega - \varepsilon_F(k) + i\eta} \\ b(\mathbf{k},-\omega) &= \frac{\rho_0 S(k)\tilde{U}_e(\mathbf{k},\omega)}{-\hbar\omega - \varepsilon_F(k) + i\eta} = a(\mathbf{k},-\omega) \end{aligned} \tag{181}$$

The last equality follows from the fact that the external potential is an even function of ω and we have changed the notation of the small imaginary term $\hbar\eta\to\eta\to 0+$.

The physical density needed for the linear response function must be a real function. We get it from Eq. (180) by adding the complex conjugate of $\delta\tilde{\rho}(\mathbf{k},t)$ and dividing by two.

$$\begin{aligned} \Re e[\delta\rho(\mathbf{k};t)] = \frac{1}{2}e^{\eta t}\Big\{ & e^{-i\omega t}\left[a(\mathbf{k},\omega) + a^*(\mathbf{k},-\omega)\right] \\ & + e^{i\omega t}\left[a(\mathbf{k},-\omega) + a^*(\mathbf{k},\omega)\right]\Big\}\,. \end{aligned} \tag{182}$$

This separates the response into the *retarded and advanced components*. The first one is analytic in the upper half of the complex ω plane and the second term in the lower half. Eq. (182) defines the Fourier components

$$\Re e[\delta\rho(\mathbf{k},\omega)] = a(\mathbf{k},\omega) + a^*(\mathbf{k},-\omega) \tag{183}$$

The retarded component with $e^{-i\omega t}$ describes a physical, causal pertubation, which propagates forward in time and the disturbance happens before the response. That is the component we need to consider here.

This defines the *Feynman approximation* of the linear response function,

$$\begin{aligned}\chi(k,\omega) &= \frac{a(\mathbf{k},\omega) + a^*(\mathbf{k},-\omega)}{\rho_0 \tilde{U}_{\rm e}(k,\omega)} \\ &= S(k)\left[\frac{1}{\hbar\omega - \varepsilon_F(k) + i\eta} - \frac{1}{\hbar\omega + \varepsilon_F(k) + i\eta}\right],\end{aligned} \tag{184}$$

which has the desired symmetry

$$\chi(k,\omega) = \chi^*(k,-\omega) \tag{185}$$

as derived from the spectral representation Eq. (125).

The positive frquency poles determine the collective excitation mode of the system, known as the Feynman approximation

$$\hbar\omega = \varepsilon_F(k) = \frac{\hbar^2 k^2}{2mS(k)} \tag{186}$$

and in the limit $\omega' = 0$ we obtain the static response function

$$\chi(k,0) = -\frac{4mS^2(k)}{\hbar^2 k^2}\,. \tag{187}$$

In liquid ^{4}He (and, in fact, also in systems where the particles interact through the screened Coulomb, or Yukawa, interaction), the excitation mode is linear in the long–wavelength limit and proportional to the speed of sound c,

$$\varepsilon_F \to \hbar k c\ ,\ \text{as}\ \ k \to 0\,. \tag{188}$$

Then the structure function must also be linear at low momenta,

$$S(k) \to \frac{\hbar k}{2mc}\ ,\ \text{as}\ \ k \to 0\,, \tag{189}$$

as pointed out earlier in Eq. (94), and the inverse of the static response function determines the incompressibility

$$-\chi^{-1}(k,0) \to mc^2\,. \tag{190}$$

Due to the long range of the Coulomb interaction, the long wavelength limits in charged systems depend strongly on the dimensionality of the system. For example, there is a gap in the three–dimensional plasmon spectrum contrary to the two–dimensional case. That is to say, in a three–dimensional system (regardless of the statistics) the energy of the collective excitation does not go to zero at low momenta but to a constant known as the plasma frequency and the static structure function becomes quadratic in the long wavelength limit pointed out in Eq. (95).

Everything put together, we have now solved our original problem: the imaginary part of the density–density response function in the single Feynman pole approximation and using Eq. (130) we get the dynamic structure function (126)

$$S(k,\omega) = S(k)\delta(\hbar\omega - \varepsilon_F(k))\,. \tag{191}$$

The strength of the pole is given by $Z(k) = S(k)$. The fact that $S(k,\omega)$ consists only of a single non–decaying excitation branch is where the Feynman approximation misses much of the physics. The Feynman approximation gives results that are exact in the long wavelength limit, but in the roton region the excitation energy is too large by a factor of two. Further more, the single–mode spectrum does not have an upper limit with increasing wave number, contrary to what is observed.[83] We return to these points when we discuss our results for the dynamic structure.

The elementary excitation modes of the system can also be obtained directly by setting $U_{ext} = 0$ in the continuity equations. Working still within the Feynman approximation and using the results (173) and (175), we get the differential equation

$$\frac{\hbar\rho_0}{2mi}\nabla_1^2\delta u_1(\mathbf{r}_1;\omega) - i\omega\Big[\rho_0\delta u_1(\mathbf{r}_1;\omega) + \rho_0^2\int d^3r_2\,[g(\mathbf{r}_1,\mathbf{r}_2)-1]\,\delta u_1(\mathbf{r}_2;\omega)\Big] = 0\,. \tag{192}$$

This has the solution (186) with

$$\delta u_1(\mathbf{r}_1;\omega = \varepsilon_F(k)) = e^{i\mathbf{k}\cdot\mathbf{r}_1}\,. \tag{193}$$

The excitation operator now takes the Feynman form,

$$\delta U = \sum_j \delta u_1(\mathbf{r}_j;\omega) = \sum_j e^{i\mathbf{k}\cdot\mathbf{r}_j}\,. \tag{194}$$

The full excitation operator of Eq. (143) can then be viewed as a generalization of this phonon–creation operator.

7 CBF–approximation

The next step is to allow also the two–particle correlation function to vary with time. Then the response of the system as a solution of the one-body continuity

equation (161) gains an additional term called *self-energy* $\Sigma(k,\omega)$, where all contributions from the time dependence of the two–particle correlation function are collected,

$$a(k,\omega) = \frac{2S(k)\rho_0\tilde{U}_{\rm ext}(\mathbf{k},\omega)}{\hbar\omega - \varepsilon_F(k) - \Sigma(k,\omega) + i\eta}\,. \tag{195}$$

Following the derivation of the linear response function leading to Eq. (185) we can write the linear response function in the same form as in Eq.(128),

$$\chi(k,\omega) = S(k)\left[\frac{1}{\hbar\omega - \varepsilon_F(k) - \Sigma(k,\omega) + i\eta} - \frac{1}{\hbar\omega + \varepsilon_F(k) + \Sigma^*(k,-\omega) + i\eta}\right]. \tag{196}$$

Collecting results of Eqs. (166), (163) and (169) for the one-body continuity equation

$$\nabla_1 \cdot \mathbf{j}_1(\mathbf{r}_1;t) + \delta\dot{\rho}_1(\mathbf{r}_1;t) = D_1(\mathbf{r}_1;t) \tag{197}$$

we find that both the density fluctuations and currents depend on the time-dependent two particle correlation function. Further more a new quantity, the triplet distribution function $g_3(\mathbf{r}_1,\mathbf{r}_2,\mathbf{r}_3)$, appears in the equation. There are systematic ways the approximate that in terms of the Abe- diagrams, but here we include only the first set of diagrams called the convolution approximation. In that approximation the emphasis is put on the correct long-range behavior.

7.1 Convolution approximation

The simplest set of diagrams needed for the triplet distribution function $g_3(\mathbf{r}_1,\mathbf{r}_2,\mathbf{r}_3)$ contains the *fan diagrams* shown in Fig. 13.

In the algebraic form it becomes

$$\begin{aligned} g_3(\mathbf{r}_1,\mathbf{r}_2,\mathbf{r}_3) &= 1 + h(\mathbf{r}_1,\mathbf{r}_2) + h(\mathbf{r}_1,\mathbf{r}_3) + h(\mathbf{r}_2,\mathbf{r}_3) \\ &+ h(\mathbf{r}_1,\mathbf{r}_2)h(\mathbf{r}_1,\mathbf{r}_3) + h(\mathbf{r}_1,\mathbf{r}_2)h(\mathbf{r}_2,\mathbf{r}_3) \\ &+ h(\mathbf{r}_1,\mathbf{r}_3)h(\mathbf{r}_2,\mathbf{r}_3) \\ &+ \int d^3r_4 h(\mathbf{r}_1,\mathbf{r}_4)h(\mathbf{r}_2,\mathbf{r}_4)h(\mathbf{r}_3,\mathbf{r}_4) \\ &+ \text{ terms with triplet correlations functions}\,. \end{aligned} \tag{198}$$

Here we have also introduced the short–hand notation $h(\mathbf{r}_1,\mathbf{r}_2) = g_2(\mathbf{r}_1,\mathbf{r}_2) - 1$. After the Fourier transform this simplifies to a product form

$$\begin{aligned} \mathcal{F}[g_3(\mathbf{r}_1,\mathbf{r}_2,\mathbf{r}_3) - 1] &= S(\mathbf{k}_1)S(\mathbf{k}_2)S(\mathbf{k}_3) \\ &\times [1 + u_3(\mathbf{k}_1,\mathbf{k}_2,\mathbf{k}_3)] - 1\,. \end{aligned} \tag{199}$$

We ignore triplet correlations for a moment, but they can be add later at will.

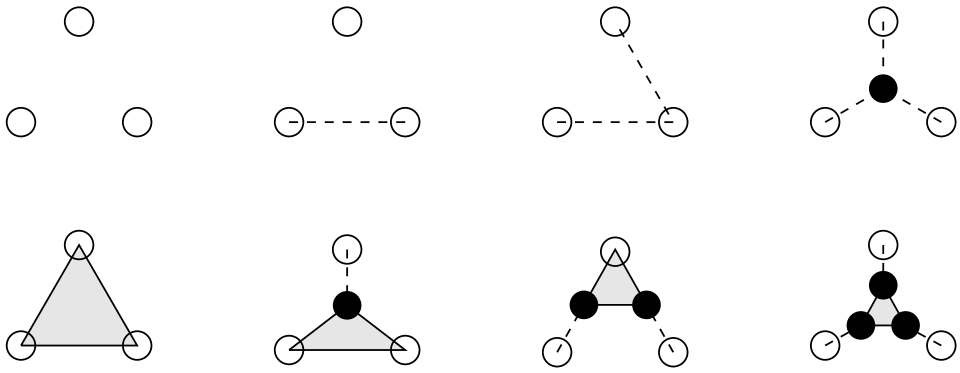

Figure 13: Convolution approximation of $g_3(\mathbf{r}_1, \mathbf{r}_2, \mathbf{r}_3)$. Circles are particle positions, black circles are integrated and open circles not. Dashed lines are functions $h(\mathbf{r}_1, \mathbf{r}_2)$ and triangles are triplet correlation functions $u_3(\mathbf{r}_1, \mathbf{r}_2, \mathbf{r}_3)$, which can be ignored in the simplest approximation. The second, third, sixth and seventh diagrams have three of the same kind, but with different particle coordinates.

7.2 One–particle equation

Let us now return to the one-particle continuity equation (161) and to the one–particle current (166). We want again to remove $\delta u_1(\mathbf{r}_1; t)$ in favor of $\delta\rho_1(\mathbf{r}_1; t)$ within the convolution approximation. In that approximation the one–particle density (163) can be written in the form

$$\delta\rho_1(\mathbf{r}_1; t) = \rho_0\ \delta v_1(\mathbf{r}_1; t) + \rho_0^2 \int d^3r_2 h(\mathbf{r}_1, \mathbf{r}_2)\delta v_1(\mathbf{r}_2; t) \tag{200}$$

with

$$\begin{aligned} \delta v_1(\mathbf{r}_1; t) &= \delta u_1(\mathbf{r}_1; t) \\ &+\rho_0 \int d^3r_2 g_2(\mathbf{r}_1, \mathbf{r}_2)\delta u_2(\mathbf{r}_1, \mathbf{r}_2; t) \\ &+\frac{1}{2}\rho_0^2 \int d^3r_2 d^3r_3 Y(\mathbf{r}_2, \mathbf{r}_3; \mathbf{r}_1)\delta u_2(\mathbf{r}_2, \mathbf{r}_3; t)\Big] , \end{aligned} \tag{201}$$

with $Y(\mathbf{r}_1, \mathbf{r}_2; \mathbf{r}_3) = h(\mathbf{r}_1, \mathbf{r}_3)h(\mathbf{r}_2, \mathbf{r}_3)$.

Eq. (200) can then be readily solved for $\delta v_1(\mathbf{r}_1; t)$

$$\rho_0\delta v_1(\mathbf{r}_1; t) = \delta\rho_1(\mathbf{r}_1; t) - \rho_0 \int d^3r_2 X(\mathbf{r}_1, \mathbf{r}_2)\delta\rho_1(\mathbf{r}_2; t)\,. \tag{202}$$

From that we can solve the one–particle correlation function,

$$\rho_0\delta u_1(\mathbf{r}_1; t) = \delta\rho_1(\mathbf{r}_1; t)$$

$$
\begin{aligned}
&-\rho_0 \int d^3r_2 X(\mathbf{r}_1,\mathbf{r}_2)\delta\rho_1(\mathbf{r}_2;t) \\
&-\rho_0^2 \int d^3r_2 g_2(\mathbf{r}_1,\mathbf{r}_2)\delta u_2(\mathbf{r}_1,\mathbf{r}_2;t) \\
&-\frac{1}{2}\rho_0^3 \int d^3r_2 d^3r_3 Y(\mathbf{r}_2,\mathbf{r}_3;\mathbf{r}_1)\delta u_2(\mathbf{r}_2,\mathbf{r}_3;t)\,.
\end{aligned}
\tag{203}
$$

Taking its gradient and inserting into equation (166) we get the one–particle current

$$
\begin{aligned}
&\mathbf{j}_1(\mathbf{r}_1;t) = \\
&= \frac{\hbar}{2mi}\Bigg\{\nabla_1\left[\delta\rho_1(\mathbf{r}_1;t) - \rho_0\int d^3r_2 X(\mathbf{r}_1,\mathbf{r}_2)\delta\rho_1(\mathbf{r}_2;t)\right] \\
&-\rho_0^2\int d^3r_2\delta u_2(\mathbf{r}_1,\mathbf{r}_2;t)\nabla_1 g_2(\mathbf{r}_1,\mathbf{r}_2) \\
&-\frac{1}{2}\rho_0^3\int d^3r_2 d^3r_3\nabla_1 Y(\mathbf{r}_1,\mathbf{r}_2;\mathbf{r}_3)\delta u_2(\mathbf{r}_2,\mathbf{r}_3;t)\Bigg\}\,.
\end{aligned}
\tag{204}
$$

We can now collect the expressions for the current and density from Eqs. (204) and (203) and insert them into the continuity equation (161). In momentum space it has the form

$$
\begin{aligned}
&[\hbar\omega - \varepsilon_{\mathrm{F}}(k)]\delta\rho_1(\mathbf{k};\omega) \\
&\qquad + \frac{\hbar^2k^2}{4m}\int\frac{d^3p}{(2\pi)^3\rho_0}\sigma_{\mathbf{k}}(\mathbf{p})\delta u_2(\mathbf{k},\mathbf{p};\omega) \\
&\qquad = 2\rho_0 S(k)U_{ext}(k,\omega)
\end{aligned}
\tag{205}
$$

where we have introduced the notation $\sigma_{\mathbf{k}}(\mathbf{p})$,

$$
\begin{aligned}
\sigma_{\mathbf{k}}(\mathbf{p}) = &-\frac{1}{k^2}\left[\mathbf{k}\cdot\left(\tfrac{\mathbf{k}}{2}+\mathbf{p}\right)S\left(\left|\tfrac{\mathbf{k}}{2}-\mathbf{p}\right|\right) + (\mathbf{p}\leftrightarrow-\mathbf{p})\right] \\
&+ S\left(\left|\tfrac{\mathbf{k}}{2}+\mathbf{p}\right|\right)S\left(\left|\tfrac{\mathbf{k}}{2}-\mathbf{p}\right|\right)\,.
\end{aligned}
\tag{206}
$$

7.3 Two–particle equation

Our aim is to get an approximation for $\delta u_2(\mathbf{r}_1,\mathbf{r}_2;t)$ using Eq. (163). The simplest term to approximate is $D_2(\mathbf{r}_1,\mathbf{r}_2;t)$ in Eq. (170) using the convolution approximation (199)

$$
D_2(\mathbf{r}_1,\mathbf{r}_2;t) = \rho_0\Big\{g_2(\mathbf{r}_1,\mathbf{r}_2)\left(D_1(\mathbf{r}_1;t) + D_1(\mathbf{r}_2;t)\right)
$$

$$+\frac{2\rho_0^2}{i\hbar}\int d^3r_3 U_{\rm ext}(\mathbf{r}_3;t)\Big[h(\mathbf{r}_1,\mathbf{r}_3)h(\mathbf{r}_2,\mathbf{r}_3) \tag{207}$$
$$+\int h(\mathbf{r}_1,\mathbf{r}_4)h(\mathbf{r}_2,\mathbf{r}_4)h(\mathbf{r}_3,\mathbf{r}_4)\Big]\Big\}.$$

The last two lines can be written in the form

$$\rho_0\int d^3r_3 Y(\mathbf{r}_1,\mathbf{r}_2;\mathbf{r}_3)D_1(\mathbf{r}_3;t) \tag{208}$$

The triplet correlation function will give an additional contribution to that. We can express now the two particle driving term entirely in terms of $D_1(\mathbf{r};t)$.

$$D_2(\mathbf{r}_1,\mathbf{r}_2;t)=\rho_0\Big\{g_2(\mathbf{r}_1,\mathbf{r}_2)\left(D_1(\mathbf{r}_1;t)+D_1(\mathbf{r}_2;t)\right)$$
$$+\rho_0\int d^3r_3 Y(\mathbf{r}_1,\mathbf{r}_2;\mathbf{r}_3)D_1(\mathbf{r}_3;t)\Big\}. \tag{209}$$

Similarly we can write the expression for the time dependent two–particle density using Eqs. (159) and (163)

$$\delta\rho_2(\mathbf{r}_1,\mathbf{r}_2;t)=\rho_0\Big\{g_2(\mathbf{r}_1,\mathbf{r}_2)\left(\delta\rho_1(\mathbf{r}_1;t)+\delta\rho_1(\mathbf{r}_2;t)\right)$$
$$+\rho_0\int d^3r_3 Y(\mathbf{r}_1,\mathbf{r}_2;\mathbf{r}_3)\delta\rho_1(\mathbf{r}_3;t)\Big\}$$
$$+\rho_0^2 g_2(\mathbf{r}_1,\mathbf{r}_2)\delta u_2(\mathbf{r}_1,\mathbf{r}_2;t)+\mathcal{F}[\delta u_2] \tag{210}$$

where we have removed the dependence on $\delta u_1(\mathbf{r},t)$ in favor of $\delta\rho_1(\mathbf{r},t)$. The functional $\mathcal{F}[\delta u_2]$ contains all the rest of the terms with $\delta u_2(\mathbf{r}_1,\mathbf{r}_2;t)$. They can be written explicitly using the definition (159), but they are not included in the CBF–approximation.

The two particle current has a term with one–particle current, but also structure which comes from the time–dependent two–particle correlations,

$$\mathbf{j}_2(\mathbf{r}_1,\mathbf{r}_2;t)=\rho_0 g_2(\mathbf{r}_1,\mathbf{r}_2)\,\mathbf{j}_1(\mathbf{r}_1;t)$$
$$+\frac{\hbar\rho_0^2}{2mi}\Big\{g_2(\mathbf{r}_1,\mathbf{r}_2)\nabla_1\delta u_2(\mathbf{r}_1,\mathbf{r}_2;t)$$
$$+\rho_0\int d^3r_3\left[g_3(\mathbf{r}_1,\mathbf{r}_2,\mathbf{r}_3)-g_2(\mathbf{r}_1,\mathbf{r}_2)g_2(\mathbf{r}_1,\mathbf{r}_3)\right]$$
$$\times\nabla_1\delta u_2(\mathbf{r}_1,\mathbf{r}_3;t)\Big\}. \tag{211}$$

The final steps of the derivation are the approximations necessary to bring the two–body equation in a numerically tractable form. Our scheme follows the general strategy of the uniform limit approximation [59] which has been

quite successful for the calculation of the optimal static three–body correlations [84, 85, 86]. The essence of the approximation is to consider *all products of two or more two–body functions small in coordinate space.*

In our specific case, the uniform limit approximation amounts to taking $g_2(\mathbf{r}_1,\mathbf{r}_2)\delta u_2(\mathbf{r}_1,\mathbf{r}_2;t) \approx \delta u_2(\mathbf{r}_1,\mathbf{r}_2;t)$ and a similar expression for $\nabla_1\delta u_2(\mathbf{r}_1,\mathbf{r}_2;t)$. While this approximation places more emphasis on the structure of $\delta u_2(\mathbf{r}_1,\mathbf{r}_2)$ it is physically appealing since it simply removes the *redundant* relevant short–range structure shared by $g_2(\mathbf{r}_1,\mathbf{r}_2)$ and $\delta u_2(\mathbf{r}_1,\mathbf{r}_2)$. Invoking the equivalent uniform limit for the three–body distribution function, the terms in Eq. (211) which depend on $\delta u_2(\mathbf{r}_1,\mathbf{r}_2;t)$ become

$$\begin{aligned}
&\frac{\hbar\rho_0^2}{2mi}\Big[g_2(\mathbf{r}_1,\mathbf{r}_2)\nabla_1\delta u_2(\mathbf{r}_1,\mathbf{r}_2;t) \\
&+\rho_0\int d^3r_3\nabla_1\delta u_2(\mathbf{r}_1,\mathbf{r}_3;t) \\
&\times\left[g_3(\mathbf{r}_1,\mathbf{r}_2,\mathbf{r}_3)-g_2(\mathbf{r}_1,\mathbf{r}_3)g_2(\mathbf{r}_1,\mathbf{r}_2)\right]\Big] \\
&\approx\frac{\hbar\rho_0^3}{2mi}\int d^3r_3\left[\delta(\mathbf{r}_3-\mathbf{r}_2)+h(\mathbf{r}_3,\mathbf{r}_2)\right]\nabla_1\delta u_2(\mathbf{r}_1,\mathbf{r}_3;t)\,.
\end{aligned} \tag{212}$$

We can now put together the approximate two–particle continuity equation

$$\begin{aligned}
&\nabla_1\cdot\Big[g_2(\mathbf{r}_1,\mathbf{r}_2)\;\mathbf{j}_1(\mathbf{r}_1;t) \\
&\quad+\frac{\hbar\rho_0^2}{2mi}\int d^3r_3\left[\delta(\mathbf{r}_3-\mathbf{r}_2)+h(\mathbf{r}_3,\mathbf{r}_2)\right]\nabla_1\delta u_2(\mathbf{r}_1,\mathbf{r}_3)\Big] \\
&\quad+\text{ same with }\;(1\leftrightarrow 2) \\
&=\;g_2(\mathbf{r}_1,\mathbf{r}_2)\Big(D_1(\mathbf{r}_1;t)-\delta\dot\rho_1(\mathbf{r}_1;t) \\
&\quad+D_1(\mathbf{r}_2;t)-\delta\dot\rho_1(\mathbf{r}_2;t)\Big) \\
&\quad+\;\rho_0\int d^3r_3 Y(\mathbf{r}_1,\mathbf{r}_2;\mathbf{r}_3)\left(D_1(\mathbf{r}_3;t)-\delta\dot\rho_1(\mathbf{r}_3;t)\right) \\
&\quad+\rho_0\delta\dot u_2(\mathbf{r}_1,\mathbf{r}_2;t)\,.
\end{aligned} \tag{213}$$

From the terms containing the time derivative $\delta\dot u_2(\mathbf{r}_1,\mathbf{r}_2;t)$ we have kept only the leading term in accordance with the uniform limit approximation and left out the term $\mathcal{F}[\delta\dot u_2]$.

If we furthermore use the one–particle continuity equation to replace the one–particle quantities with one–particle currents we arrive at our final approximate form

$$\begin{aligned}
&\Big[\frac{\hbar\rho_0^2}{2mi}\int d^3r_3\left[\delta(\mathbf{r}_3-\mathbf{r}_2)+h(\mathbf{r}_3,\mathbf{r}_2)\right]\nabla_1^2\delta u_2(\mathbf{r}_1,\mathbf{r}_3;t) \\
&+\text{same with }\;(1\leftrightarrow 2)\Big]-\rho_0\delta\dot u_2(\mathbf{r}_1,\mathbf{r}_2;t)
\end{aligned} \tag{214}$$

$$= \mathbf{j}_1(\mathbf{r}_1;t)\cdot\nabla_1 g_2(\mathbf{r}_1,\mathbf{r}_2) + \mathbf{j}_1(\mathbf{r}_2;t)\cdot\nabla_2 g_2(\mathbf{r}_1,\mathbf{r}_2)$$
$$+ \rho_0\int d^3r_3 Y(\mathbf{r}_1,\mathbf{r}_2;\mathbf{r}_3)\nabla_3\cdot\mathbf{j}_1(\mathbf{r}_3;t)\,.$$

The last step is to decouple the equations of motion. We can do this by approximating the one–particle current, given in Eq. (166) by the Feynman current of Eq. (173)

$$\mathbf{j}(\mathbf{r}_1;t) = \frac{\hbar\rho_0}{2mi}\nabla_1\delta u_1(\mathbf{r}_1;t) \tag{215}$$
$$= \frac{\hbar\rho_0}{2mi}\nabla_1\left[\delta\rho_1(\mathbf{r}_1;t) - \rho_0\int d^3r_2 X(\mathbf{r}_1,\mathbf{r}_2)\delta\rho_1(\mathbf{r}_2;t)\right]\,.$$

On the second line we have solved $\delta u_1(\mathbf{r}_1;t)$ in terms of $\delta\rho_1(\mathbf{r}_1;t)$ from Eq. (175) using the direct correlation function $X(\mathbf{r}_1,\mathbf{r}_2)$.

The fluctuating two–particle correlation function can now be expressed, in closed form, as a functional of one–body quantities alone. The integrals in Eq. (214) are of convolution form and can be integrated in momentum space leading to the result

$$\left[\hbar\omega - \varepsilon_{\rm F}\left(\left|\tfrac{\mathbf{k}}{2}+\mathbf{p}\right|\right) - \varepsilon_{\rm F}\left(\left|\tfrac{\mathbf{k}}{2}-\mathbf{p}\right|\right)\right]$$
$$\times S\left(\left|\tfrac{\mathbf{k}}{2}+\mathbf{p}\right|\right) S\left(\left|\tfrac{\mathbf{k}}{2}-\mathbf{p}\right|\right)\delta u_2(\mathbf{k},\mathbf{p};\omega)$$
$$+ \varepsilon_{\rm F}(k)\;\sigma_{\mathbf{k}}(\mathbf{p})\;\delta\rho_1(\mathbf{k};\omega) = 0 \tag{216}$$

where $\sigma_{\mathbf{k}}(\mathbf{p})$ is defined in Eq. (206). It is now evident that we can solve from Eq. (216) the fluctuating two–body correlation function directly in terms of the one–body density fluctuation,

$$\frac{\delta u_2(\mathbf{k},\mathbf{p};\omega)}{\delta\rho_1(\mathbf{k};\omega)} = -\frac{\varepsilon_{\rm F}(k)\sigma_{\mathbf{k}}(\mathbf{p})\left[S\left(\left|\tfrac{\mathbf{k}}{2}+\mathbf{p}\right|\right) S\left(\left|\tfrac{\mathbf{k}}{2}-\mathbf{p}\right|\right)\right]^{-1}}{\hbar\omega - \varepsilon_{\rm F}\left(\left|\tfrac{\mathbf{k}}{2}+\mathbf{p}\right|\right) - \varepsilon_{\rm F}\left(\left|\tfrac{\mathbf{k}}{2}-\mathbf{p}\right|\right)}\,, \tag{217}$$

needed for the self–energy.

7.4 The self–energy and the linear response function

As the final step we define the self–energy by dividing the left hand side of Eq. (205) with $\delta\rho_1(\mathbf{k};\omega)$. That gives the result

$$\left[\hbar\omega - \varepsilon_{\rm F}(k) - \Sigma(\mathbf{k},\omega)\right]\delta\rho_1(\mathbf{k};\omega) = 2\rho_0 S(k) U_{ext}(k,\omega) \tag{218}$$

from which the self–energy emerges

$$\Sigma(\mathbf{k},\omega) = -\frac{\hbar^2k^2}{4m}\int\frac{d^3p}{(2\pi)^3\rho_0}\sigma_{\mathbf{k}}(\mathbf{p})\frac{\delta u_2(\mathbf{k},\mathbf{p};\omega)}{\delta\rho_1(\mathbf{k};\omega)}\,. \tag{219}$$

But the ratio $\delta u_2(\mathbf{k},\mathbf{p};\omega)/\delta\tilde{\rho}_1(\mathbf{k};\omega)$ was exactly what we got out of the two–body equation (217) in closed form. The expression of the self–energy turns into an more familiar form [63] if we change the variables $\frac{\mathbf{k}}{2}+\mathbf{p}\rightarrow-\mathbf{p}$ and $\frac{\mathbf{k}}{2}-\mathbf{p}\rightarrow-\mathbf{q}$ and then introduce the Dirac δ–function to insure the momentum conservation, $\mathbf{p}+\mathbf{q}+\mathbf{k}=0$,

$$\Sigma(k,\omega)=\frac{1}{2}\int\frac{d^3p\;d^3q}{(2\pi)^3\rho_0}\delta(\mathbf{k}+\mathbf{p}+\mathbf{q})\frac{|V_3(\mathbf{k};\mathbf{p},\mathbf{q})|^2}{\hbar\omega-\varepsilon_{\rm F}(p)-\varepsilon_{\rm F}(q)} \tag{220}$$

where the three–plasmon/phonon coupling matrix element

$$\begin{aligned}V_3(\mathbf{k};\mathbf{p},\mathbf{q})&=-\frac{\hbar^2}{2m}\frac{1}{\sqrt{S(p)S(q)S(k)}}\\&\times\left[\mathbf{k}\cdot\mathbf{p}S(p)+\mathbf{k}\cdot\mathbf{q}S(q)+k^2S(p)S(q)\right]\\&=\frac{\hbar^2}{2m}\sqrt{\frac{S(p)S(q)}{S(k)}}\left[\mathbf{k}\cdot\mathbf{p}\tilde{X}(p)+\mathbf{k}\cdot\mathbf{q}\tilde{X}(q)\right]\end{aligned} \tag{221}$$

is given in terms of the ground–state structure function $S(k)$, the direct correlation function $\tilde{X}(k)=1-S(k)^{-1}$.

Using the derivation of the linear response function presented in connection with the Feynman approximation leading to Eq. (185) we can write $\chi(k,\omega)$ as in Eq. (128).

$$\begin{aligned}\chi(k,\omega)=S(k)\Big[&\frac{1}{\hbar\omega-\varepsilon(k)-\Sigma(k,\omega)}\\&-\frac{1}{\hbar\omega+\varepsilon(k)+\Sigma^*(k,-\omega)}\Big].\end{aligned} \tag{222}$$

We are studying excitations at zero temperature with positive frequencies $\omega>0$ and from the fluctuation-dissipation theorem (126) we get the dynamic structure function,

$$\begin{aligned}S(k,\omega)&=-\frac{1}{\pi}\Im m\left[\chi(k,\omega)\right]\\&=-\frac{1}{\pi}\Im m\left[\frac{S(k)}{\hbar\omega-\varepsilon_F(k)-\Sigma(k,\omega)}\right].\end{aligned} \tag{223}$$

7.5 Numerical evaluation of the self–energy

The integrand in the expression of the self–energy in Eq. (220) can have poles, which makes the self–energy a complex function. Let us look next in detail how it can be calculated numerically. After integrating the δ–function and the

ϕ–coordinate we are left with the double integral

$$\Sigma(k,\omega) = \frac{1}{2}\frac{1}{(2\pi)^2\rho_0}\int_0^\infty q^2 dq \times \int_{-1}^{1} dx \frac{|V_3(k;q,x)|^2}{\hbar\omega - \varepsilon_{\rm F}(|\mathbf{k}+\mathbf{q}|) - \varepsilon_{\rm F}(q)} \tag{224}$$

where we have chosen the following variables

$$\begin{aligned} \mathbf{p} &= -(\mathbf{k}+\mathbf{q}) \\ p^2 &= k^2 + 2\mathbf{k}\cdot\mathbf{q} + q^2 = k^2 + q^2 + 2kqx \\ x &= \frac{p^2 - k^2 - q^2}{2kq}\,. \end{aligned} \tag{225}$$

Replacing x with p we can write the integral in the form

$$\Sigma(k,\omega) = \frac{1}{8\pi^2\rho_0 k}\int_0^\infty q dq \times \int_{|k-q|}^{k+q} p dp \frac{|V_3(k;q,p)|^2}{\hbar\omega - \varepsilon_{\rm F}(p) - \varepsilon_{\rm F}(q)}\,. \tag{226}$$

This integral has a pole when

$$\hbar\omega = \varepsilon_{\rm F}(p) + \varepsilon_{\rm F}(q)\,. \tag{227}$$

In other words when the energy of the excitation is equal to the energy of two elementary Feynman modes. In such a case the self–energy becomes a complex function.

Assuming that this pole is the only pole in the integrand and that the integrand converges fast enough at infinity we can separate the real and imaginary parts

$$\Sigma(k,\omega) = \Delta(k,\omega) - i\Gamma(k,\omega) \tag{228}$$

by remembering that

$$\frac{1}{\omega' - \omega} = \mathcal{P}\frac{1}{\omega' - \omega} - i\pi\delta(\omega' - \omega)\,. \tag{229}$$

The imaginary part can then be calculated with one integration only

$$\Gamma(k,\omega) = \frac{1}{8\pi\rho_0 k}\int_0^\infty q dq \int_{|k-q|}^{k+q} p dp \times |V_3(k;q,p)|^2 \delta(\hbar\omega - \varepsilon_{\rm F}(p) - \varepsilon_{\rm F}(q))\,. \tag{230}$$

The real part could be calculated from the above principle value integral, but it is much more convenient for numerics to calculate it from the imaginary part

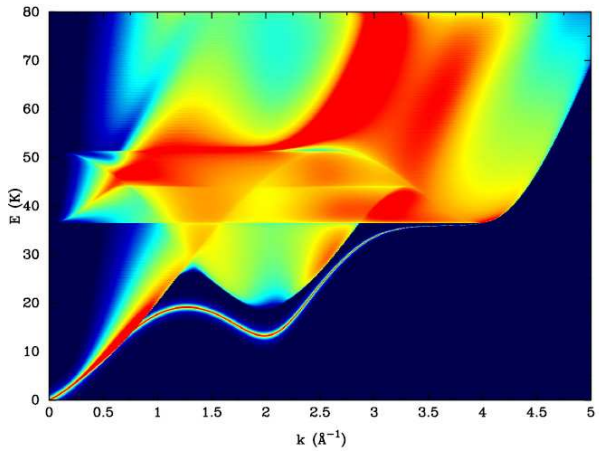

Figure 14: $S(k, w)$ for helium at the saturation density.

using Kramers–Kronig relations which connect the real and imaginary parts. If $f(\omega)$ is an analytic complex function

$$f(\omega) = a(\omega) + ib(\omega) \tag{231}$$

then

$$\begin{aligned} a(\omega) &= \frac{1}{\pi}\mathcal{P}\int_{-\infty}^{\infty} d\omega' \frac{b(\omega')}{\omega' - \omega} \\ b(\omega) &= -\frac{1}{\pi}\mathcal{P}\int_{-\infty}^{\infty} d\omega' \frac{a(\omega')}{\omega' - \omega}\,. \end{aligned} \tag{232}$$

Provided that $a(\omega)$ and $b(\omega)$ converge fast enough at large ω.

Using the first relation we can write the real part of the self–energy in the form

$$\Delta(k, \omega) = -\frac{1}{\pi}\mathcal{P}\int_{0}^{\infty} d\omega' \frac{\Gamma(k, \omega')}{\omega' - \omega}\,. \tag{233}$$

The imaginary part is non–zero only when $\omega' > 0$. In the numerical integration of the principle value one distributes the integration mesh symmetrically around ω and leaves out the point $\omega' = \omega$.

8 Summary

The variational Jastrow–Feenberg theory provides a powerful theoretical tool in obtaining microscopic understanding of the many–particle structure and processes present in strongly–correlated quantum fluids. A detailed derivation of

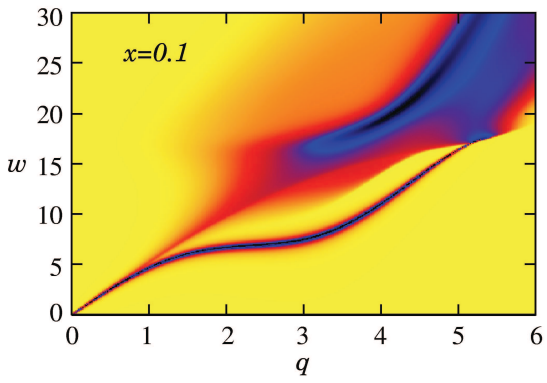

Figure 15: $S(k, w)$ for a hard core potential at $x = 0.1$.

the optimized ground state and the equations of motions for the dynamic system have been described. By extending the time dependence to two–particle correlations and, hence, including three–phonon processes we went beyond the conventional Feynman theory of excitations. We showed that the CBF approximation gives qualitatively reasonable results for the dynamic structure. We studied the analytic properties of the dynamic structure function and made a clear distinction between the real elementary–excitation mode and the broader complex mode, which can decay into elementary excitations.

References

[1] H. Kammerlingh Onnes, Proc. R. Acad. Amsterdam **11**, 168 (1908).

[2] J. Wilks, *The properties of Liquid and Solid Helium* (Clarendon Press, Oxford,1967).

[3] *The Physics of Liquid and Solid Helium*, edit. by K. H. Bennemann and J. B. Ketterson, (John Wiley & Sons, New York, 1976).

[4] J. Wilks and D. S. Betts, *An Introduction to Liquid Helium* (Clarendon Press, Oxford, 1987).

[5] H. R. Glyde, *Excitations in Liquid and Solid Helium*, (Clarendon Press, Oxford, 1994).

[6] P. L. Kapitza, Nature (London) **141**,74 (1938).

[7] J. F. Allen and H. Jones, Nature (London) **141**,75 (1938).

[8] D. D. Osheroff, R.C. Richardson, and D. M. Lee, Phys. Rev. Lett. **28**, 1098 (1972).

[9] *Excitations in Two–Dimensional and Three–Dimensional Quantum Fluids*, Vol. 257 of NATO *Advanced Study Institute, Series B: Physics,* A. F. G. Wyatt and H. J. Lauter, eds. (Plenum, New York, 1991).

[10] W. Teizer, R. B. Hallock, E. Dujardin, and T. W. Ebbesen, Phys. Rev. Lett. **82**, 5305 (1999).

[11] S. Grebenev, J. P. Toennies, and A. Vilesov, Science **279**, 2083 (1998).

[12] *Microscopic Quantum Many–Body Theories and Their Applications*, J. Navarro and A. Polls eds., Lecture Note in Physics, Vol. 510, (Springer-Verlag, Heidelberg, 1998).

[13] S. Rosati, in *International School of Physics Enrico Fermi, Course LXXIX*, edited by A. Molinari, 1981 (North-Holland, Amsterdam), 73.

[14] J. G. Zabolitzky, in *Advances in Nuclear Physics* , Vol. 12, edited by J. W. Negele and E. Vogt (Plenum, New York, 1980).

[15] C. E. Campbell, in *Progress in Liquid Physics*, edited by C.A. Croxton, Ch. 6 (Wiley, New York, 1977).

[16] J. W. Clark, in *Progress in Particle and Nuclear Physics*, Vol. 2, edited by D. H. Wilkinson, p.89 (Pergamon, Oxford, 1979).

[17] S. Rosati and S. Fantoni, in *The Many–Body Problem: Jastrow Correlations Versus Brueckner Theory*, (Lecture Notes in Physics, Vol. 138), edited by R. Guardiola and J. Ros, p. 1, (Springer, Berlin, 1981).

[18] E. Feenberg, *Theory of Quantum Fluids* (Academic Press, New York, 1969).

[19] R. A. Aziz, V. P. S. Nain, J. S. Caley, W. L. Taylor, and G. T. McConville, J. Chem. Phys. **70**, 4330 (1979).

[20] R. A. Aziz, F. R. W. McCourt, and C. C. K. Wong, Mol. Phys. **61**, 1487 (1987).

[21] R. Jastrow, Phys. Rev. **98**, 1479 (1955).

[22] H. W. Jackson and E. Feenberg, Ann. of Phys. **15**, 266 (1961).

[23] V. R. Pandharipande and H. A. Bethe, Phys. Rev. C **7**, 1312 (1973).

[24] J. W. Clark and P. Westhaus, Phys. Rev. **149**, 990 (1966).

[25] W. L. McMillan, Phys. Rev. **138**, 442 (1965).

[26] D. Schiff and L. Verlet, Phys. Rev. **160**, 208 (1967).

[27] C. E. Campbell, in *Progress in Liquid Physics*, C. A. Croxton, ed., Ch. 6, (Wiley, New York, 1977).

[28] R. T. Azuah, W. G. Stirling, H. R. Glyde, M. Bonisegni, P. E. Sokol, and S. M. Bennington, Phys. Rev. B **56**, 14620 (1997).

[29] S. Fantoni and S. Rosati, Nuovo Cimento **20A**, 179 (1974).

[30] J. P. Hansen and I. R. McDonald, *Theory of Simple Fluids* (Academic Press, New York, 1976).

[31] J. M. J. van Leeuwen, J. Groeneveld, and J. de Boer, Physica **25**, 792 (1959).

[32] J. K. Percus and G. J. Yevick, Phys. Rev. **110**, 1 (1958).

[33] Q. N. Usmani, B. Friedman, and V. R. Pandharipande, Phys. Rev. B **25**, 4502 (1982).

[34] K. Schmidt, M. H. Kalos, M. A. Lee, and G. V. Chester, Phys. Rev. Lett. **45**, 573 (1981).

[35] R. Abe, Orig. Theor. Phys. **21**, 421 (1959).

[36] Q. N. Usmani, S. Fantoni, and V. R. Pandharipande, Phys. Rev. B **26**, 6123 (1982).

[37] E. Krotscheck, Phys. Rev. B **33**, 3158 (1986).

[38] C. C. Chang and C. E. Campbell, Phys. Rev. B **15**, 4238 (1977).

[39] J. Boronat and J. Casulleras, Phys. Rev. B **49**, 8920 (1994).

[40] S. Stringari and J. Treiner, Phys. Rev. B **36**, 8369 (1987).

[41] L. Castillejo, A. D. Jackson, B. K. Jennings, and R. A. Smith, Phys. Rev. B **20**, 3631 (1979).

[42] C. E. Campbell and E. Feenberg, Phys. Rev. **188**, 346 (1969).

[43] M. Saarela, *Elementary excitations and dynamic structure of quantum fluids,* this volume.

[44] L. Landau, Phys. Rev. **60**, 356 (1941). L. Landau, J. Phys. U.S.S.R. **5**, 71, (1941).

[45] R. P. Feynman, Phys. Rev. **94**, 262 (1954).

[46] D. Pines and P. Nozières, *The Theory of Quantum Liquids*, Vol. I, (Addison Wesley, 1989).

[47] D. M. Ceperley, Rev. Mod. Phys. **67**,279 (1995).

[48] J. Boronat, in *Lecture notes in Physics: Microscopic Quantum Many-Body Theories and Their Applications*, edited by J. Navarro and A. Polls (Springer-Verlag, Berlin Heidelberg, 1998), Vol. 510, pp. 358-379.

[49] S. Moroni, S. Conti and M. P. Tosi, Phys. Rev. B **53**, 9688 (1996).

[50] A. F. G. Wyatt, M. A. H. Tucker, I. N. Adamenko, K. E. Nemchenko and A. V. Zhukov, Phys. Rev. B **62**, 9402 (2000).

[51] H. Glyde, *Excitations in liquid and solid helium* (Oxford University Press, Oxford, 1994).

[52] A. Bijl, Physica **7**, 869 (1940).

[53] L. Landau, J. Phys. U.S.S.R. **5**, 71 (1941).

[54] L. Landau, Phys. Rev. **60**, 356 (1941).

[55] L. Landau, J. Phys. U.S.S.R. **11**, 91 (1947).

[56] N. N. Bogoliubov, J. Phys. U.S.S.R **9**, 23 (1947).

[57] R. P. Feynman, Phys. Rev. **94**, 262 (1954).

[58] R. P. Feynman and M. Cohen, Phys. Rev. **102**, 1189 (1956).

[59] E. Feenberg, *Theory of Quantum Fluids* (Academic, New York, 1969).

[60] J. W. Clark, in *Progress in Particle and Nuclear Physics*, edited by D. H. Wilkinson (Pergamon Press Ltd., Oxford, 1979), Vol. 2, pp. 89–199.

[61] H. W. Jackson and E. Feenberg, Ann. Phys. (NY) **15**, 266 (1961).

[62] H. W. Jackson and E. Feenberg, Rev. Mod. Phys. **34**, 686 (1962).

[63] C. C. Chang and C. E. Campbell, Phys. Rev. B **13**, 3779 (1976).

[64] C. E. Campbell, in *Progress in Liquid Physics*, edited by C. A. Croxton (Wiley, London, 1978), Chap. 6, pp. 213–308.

[65] S. Manousakis and V. R. Pandharipande, Phys. Rev. B **30**, 5062 (1984).

[66] L. Reatto, S. A. Vitiello, and G. L. Masserini, J. Low Temp. Phys. **93**, 879 (1993).

[67] S. Moroni, L. Reatto, and S. Fantoni, Czech. J. Phys. Suppl. S1 **46**, 281 (1996).

[68] J. Boronat and J. Casulleras, Europhys. Lett. **38**, 291 (1997).

[69] V. L. Berezinskiĭ, Sov. Phys. JETP **32**, 493 (1971).

[70] J. M. Kosterlitz and D. J. Thouless, J. Phys. C **6**, 1181 (1973).

[71] R. J. Donnelly, *Quantized Vortices in Helium II* (Cambridge University Press, Cambridge, 1991).

[72] M. Saarela, B. E. Clements, E. Krotscheck, and F. V. Kusmartsev, J. Low Temp. Phys. **93**, 971 (1993).

[73] Saarela and F. V. Kusmartsev, Phys. Lett. A **202**, 317 (1995).

[74] M. Saarela, Phys. Rev. B **33**, 4596 (1986).

[75] M. Saarela and J. Suominen, in *Condensed Matter Theories*, edited by J. S. Arponen, R. F. Bishop, and M. Manninen (Plenum, New York, 1988), Vol. 3, pp. 157–165.

[76] J. Suominen and M. Saarela, in *Condensed Matter Theories*, edited by J. Keller (Plenum, New York, 1989), Vol. 4, p. 377.

[77] B. E. Clements *et al.*, Phys. Rev. B **50**, 6958 (1994).

[78] B. E. Clements, E. Krotscheck, and C. J. Tymczak, Phys. Rev. B **53**, 12253 (1996).

[79] A. D. B. Woods and R. A. Cowley, Rep. Prog. Phys. **36**, 1135 (1973).

[80] V. Apaja *et al.*, Phys. Rev. B **55**, 12925 (1997).

[81] A. K. Kerman and S. E. Koonin, Ann. Phys. (NY) **100**, 332 (1976).

[82] P. Kramer and M. Saraceno, *Geometry of the time-dependent variational principle in quantum mechanics*, Vol. 140 of *Lecture Notes in Physics* (Springer, Berlin, Heidelberg, and New York, 1981).

[83] B. Fåk and J. Bossy, J. Low Temp. Phys. **112**, 1 (1998).

[84] C. E. Campbell, Phys. Lett. A **44**, 471 (1973).

[85] C. C. Chang and C. E. Campbell, Phys. Rev. B **15**, 4238 (1977).

[86] E. Krotscheck, Phys. Rev. B **33**, 3158 (1986).

[87] H. W. Jackson, Phys. Rev. A **9**, 964 (1974).

[88] F. Dalfovo and S. Stringari, Phys. Rev. B **46**, 13991 (1992).

[89] J. Halinen, V. Apaja, and M. Saarela, J. Low Temp. Phys. (2002), in press.

[90] A. Gold, Z. Phys. B **89**, 1 (1992).

[91] R. A. Cowley and A. D. B. Woods, Can. J. Phys. **49**, 177 (1971).

[92] H. N. Robkoff and R. B. Hallock, Phys. Rev. B **24**, 159 (1981).

[93] E. H. Graf, V. J. Minkiewicz, H. B. Möller, and L. Passell, Phys. Rev. A **10**, 1748 (1974).

[94] O. W. Dietrich, E. H. Graf, C. H. Huang, and L. Passell, Phys. Rev. A **5**, 1377 (1972).

[95] V. Apaja and M. Saarela, Phys. Rev. B **57**, 5358 (1998).

[96] E. Krotscheck and M. Saarela, Physics Reports **232**, 1 (1993).

[97] R. J. Donnelly, J. A. Donnelly, and R. N. Hills, J. Low Temp. Phys. **44**, 471 (1981).

[98] A. D. B.Woods, P. A. Hilton, R. Scherm, and W. G. Stirling, J. Phys. C **10**, L45 (1977).

[99] E. C. Svensson, R. Scherm, and A. D. B.Woods, J. Phys. C **39**, 6 (1978).

[100] V. Apaja, J. Halinen, and M. Saarela, J. Low Temp. Phys. **113**, 909 (1998).

[101] V. Apaja, J. Halinen, and M. Saarela, Physica B **284-288**, 29 (2000).

[102] J. Halinen, V. Apaja, K. A. Gernoth, and M. Saarela, J. Low Temp. Phys. **121**, 531 (2000).

[103] P. R. Roach, J. B. Ketterson, and C. W. Woo, Phys. Rev. A **2**, 543 (1970).

[104] D. O. Edwards and R. C. Pandorf, Phys. Rev. A **140**, 816 (1965).

[105] S. Giorgini, J. Boronat, and J. Casulleras, Phys. Rev. B **54**, 6099 (1996).

[106] P. A. Whitlock, G. V. Chester, and M. H. Kalos, Phys. Rev. B **38**, 2418 (1988).

[107] M. C. Gordillo and D. M. Ceperley, Phys. Rev. B **58**, 6447 (1998).

[108] M. Saarela and E. Krotscheck, J. Low Temp. Phys. **90**, 415 (1993).

[109] M. Saarela, in *Recent Progress in Many Body Theories*, edited by Y. Avishai (Plenum, New York, 1990), Vol. 2, pp. 337–346.

[110] E. Krotscheck *et al.*, Phys. Rev. B **58**, 12282 (1998).

[111] J. C. Owen, Phys. Rev. B **23**, 5815 (1981).

[112] B. Fåk *et al.*, Phys. Rev. B **41**, 8732 (1990).

[113] D. S. Greywall, Phys. Rev. B **20**, 2643 (1979).

[114] J. R. Owers-Bradley *et al.*, J. Low Temp. Phys. **72**, 201 (1988).

[115] S. Yorozu, H. Fukuyama, and H. Ishimoto, Phys. Rev. B **48**, 9660 (1993).

[116] R. Simons and R. M. Mueller, Czekoslowak Journal of Physics Suppl. **46**, 201 (1996).